Food & Function

ROYAL SOCIETY OF CHEMISTRY

PAPER

View Article Online
View Journal | View Issue

Cite this: *Food Funct.*, 2023, **14**, 9650

Oligonol ameliorates liver function and brain function in the 5 × FAD mouse model: transcriptional and cellular analysis†

Danbi Jo,‡[a,b] Archana Arjunan,[a] Seoyoon Choi,[a,b] Yoon Seok Jung,[a] Jihyun Park,[c,d] Jihoon Jo,[e] Oh Yoen Kim*[c,d] and Juhyun Song *[a,b]

Alzheimer's disease (AD) is a common neurodegenerative disease worldwide and is accompanied by memory deficits, personality changes, anxiety, depression, and social difficulties. For treatment of AD, many researchers have attempted to find medicinal resources with high effectiveness and without side effects. Oligonol is a low molecular weight polypeptide derived from lychee fruit extract. We investigated the effects of oligonol in 5 × FAD transgenic AD mice, which developed severe amyloid pathology, through behavioral tests (Barnes maze, marble burying, and nestle shredding) and molecular experiments. Oligonol treatment attenuated blood glucose levels and increased the antioxidant response in the livers of 5 × FAD mice. Moreover, the behavioral score data showed improvements in anxiety, depressive behavior, and cognitive impairment following a 2-month course of orally administered oligonol. Oligonol treatment not only altered the circulating levels of cytokines and adipokines in 5 × FAD mice, but also significantly enhanced the mRNA and protein levels of antioxidant enzymes and synaptic plasticity in the brain cortex and hippocampus. Therefore, we highlight the therapeutic potential of oligonol to attenuate neuropsychiatric problems and improve memory deficits in the early stage of AD.

Received 22nd August 2023,
Accepted 29th September 2023

DOI: 10.1039/d3fo03451h

rsc.li/food-function

1. Introduction

Alzheimer's disease (AD), a common neurodegenerative disorder, is characterized by chronic neuroinflammation, progressive accumulation of amyloid beta (Aβ) plaques, and neurofibrillary tangles.[1] The pathogenesis of AD causes gradual cognitive decline and neuropsychiatric symptoms such as depressive mood and anxiety.[2–5] Some studies have suggested that more than 50% of patients with AD have neuropsychiatric symptoms such as anxiety-like behaviors.[6–9] Several studies have demonstrated that the AD brain has global damage in various regions, including the hippocampus, prefrontal cortex, limbic subcortical region, dentate gyrus, and *para* hippocampal region.[10–12] The medial temporal lobe, including the cortex and hippocampus, is associated with memory function, and the amygdala is associated with anxiety, both of which exhibit slight atrophy and accumulation of Aβ plaque in the context of AD.[13] Additionally, in AD, the brain exhibits severe oxidative stress, glial activation, neuronal cell death, and inflammation, leading to memory deficits.[14,15]

Many attempts have been made to identify the potential of various natural plant products to ameliorate the pathogenesis of AD, with relatively low side effects. Polyphenols, a remarkable antioxidant that is abundant in various plant products (fruits and vegetables), play an important role in attenuating oxidative stress,[16] improving network signaling between neurons and glia, and decreasing excessive accumulation of Aβ plaque and tau protein in the AD brain.[17] Naringin from citrus fruits has been reported to have a neuroprotective effect in AD brain cerebellum by regulating tau phosphorylation and oxidative stress.[18] Quercetin, a well-known flavonoid obtained from red berries, grapes, and onions, can increase mitochondrial biogenesis in neurons and protect neuronal cells against oxidative stress-induced free radicals.[19] In addition, polyphe-

[a]*Department of Anatomy, Chonnam National University Medical School, Seoyangro 264, Hwasun 58128, Republic of Korea. E-mail: juhyunsong@chonnam.ac.kr, danbijo0818@gmail.com, sy20180433@gmail.com, yhemm@naver.com, archanaibms@gmail.com; Fax: +82-51-200-7353, +82-61-375-5834; Tel: +82-51-200-7326, +82-61-379-2706*
[b]*Biomedical Science Graduate Program (BMSGP), Chonnam National University, Seoyangro 264, Hwasun 58128, Republic of Korea*
[c]*Department of Food Science and Nutrition, Dong-A University, Nakdong-daero 550 beon-gil, Saha-gu, Busan, 49315, Republic of Korea. E-mail: jihyun6807@naver.com, oykim@dau.ac.kr*
[d]*Department of Health Sciences, Graduate School of Dong-A University, Nakdong-daero 550 beon-gil, Saha-gu, Busan, 49315, Republic of Korea*
[e]*Department of Biomedical Science, Chonnam National University Medical School, Seoyangro 264, Hwasun 58128, Republic of Korea. E-mail: Jo@jnu.ac.kr*

†Electronic supplementary information (ESI) available. See DOI: https://doi.org/10.1039/d3fo03451h

‡These authors contributed equally to this study as corresponding authors.

nols obtained from conyza dioscoridis are known to attenuate AD pathologies,[20] while others from resveratrol have been shown to enhance memory deficit in an AD mouse model.[21]

Recently, oligonol, a low-molecular-weight polyphenol derived from lychee fruit extract and containing catechin-type monomers and pro-anthocyanidin oligomers, has gained interest owing to its potential to attenuate cognition impairment in AD and aging models.[22,23] Oliogonol has biologically beneficial effects, including anti-inflammation, anti-obesity, anticancer, and lipid regulation.[24,25] Oral administration of oligonol at a high dose (100–200 mg per kg of body weight) in amyloid β (25–35)-induced AD model mice for 2 weeks has been found to improve memory deficit and cognition impairment.[22] Moreover, in a senescence-accelerated prone mouse model (SAMP8), locomotive deficit was significantly improved and the severity of infection-induced inflammation was modulated following 36-week oligonol treatment (60 mg per kg of body weight), suggesting a benefit of oligonol in aging-associated diseases such as AD or Parkinson's disease.[23]

However, no previous study has identified the role of oligonol, a low-molecular-weight polyphenol, in metabolic conditions or cognitive function in an AD model with rapidly developing severe amyloid pathology. Therefore, in this study, we aimed to investigate whether oligonol influences liver function, cognitive decline, neuropsychiatric behaviors, and metabolic alterations in 5 × FAD mice, which rapidly develop severe amyloid pathology, a common mouse model of early stage AD.[26] Our findings highlight the therapeutic potential of oligonol as a treatment for AD in terms of metabolic enhancement and cognitive improvement.

2. Materials and methods

2.1. Animal and experimental design

Five-month-old 5 × FAD male mice (n = 6) were housed in the Laboratory Animal Research Center, Chonnam National University (CNU), under a 16 h light/8 h dark cycle at 23 °C with 60% humidity and were given *ad libitum* access to food and water when the experimental procedures were conducted. Each animal was housed in a cage. The body weight and blood glucose levels of all mice were measured once a week. The 5 × FAD mice were subdivided into two groups: oligonol treatment (n = 3) and placebo (n = 3). The oligonol treatment groups were orally administered oligonol at a dose of 50 mg kg^{-1} day^{-1} as a suspension in drinking water daily for 8 weeks. The placebo group was given water in the same way as the oligonol treatment group (ESI Fig. 1† and Fig. 1A). The experiments were performed following the recommendations of the 96 guidelines for animal experiments established by the Animal Ethics Committee at CNU. The Animal Ethics Committee approved the protocol at CNU. At the 7th week of the experiments, animals were tested in the Barnes maze, marble burying test (MBT), and nestle shredding behavior test (NST), before being sacrificed at week 8.

2.2. Barnes maze behavior test

The Barnes maze test was successfully performed on 5 × FAD mice to determine their spatial learning and memory. The Barnes maze (Jungdo Bio & Plant) is an opaque circular platform (diameter: 92 cm) with 20 equally spaced holes (diameter: 5 cm) located 2 cm from the edge. In a brightly lit environment, mice naturally seek the dark enclosed area provided by the black goal box (20 × 10 × 4 cm), which was located under the same escape hole throughout all trials. From the surface of the maze, the escape hole containing the goal box appears identical to the other 19 holes. The test was conducted in three phases: a habituation phase, lasting for 5 min (day 0); a training phase, lasting for 1–5 days; and a spatial reference memory phase, lasting for 7 days. In the training and spatial reference memory phases, the escape box was placed under one of the 20 holes. Initially, the mice were placed at the center of the maze, from which point, they explored the maze until they found the escape box. If the mice failed to enter the escape box within 240 s, the experimenter gently led them into the escape box. The mouse remained in the escape box for an additional 30 s before it was removed and returned to the home cage. To dissipate and disseminate odor cues for subsequent trials, the escape box, additional boxes, and maze surface were sprayed with 70% isopropyl alcohol and wiped non-systematically. The location of the escape box remained the same for each mouse during every trial of the training phase. The training was repeated twice a day, with a 30 min interval between each session. The performances of mice (latency: the time taken to escape box, and the number of incorrect entries) was recorded and averaged. The data were collected by a video camera located above the maze and were analyzed using ImageJ.[27]

2.3. Marble burying behavior test

The marble burying behavior test was used to assess the obsessive-compulsive behavior of 5 × FAD mice. Briefly, a polycarbonate cage (26 cm × 48 cm × 20 cm) was filled with bedding material to a depth of 5 cm and contained 20 standard glass marbles (15 mm diameter, 5.2 g in weight) in five rows of four marbles. The mice were allowed to explore the polycarbonate cage for 30 min. Water and food withheld during the experiment. Scoring was conducted when the rat buried the marble in two-thirds of its surface into the bedding material.[28]

2.4. Nestlet shredding behavior test

The polycarbonate cage (26 cm × 48 cm × 20 cm) was filled with bedding material, 1 g of nestlet (cotton bed) was kept, and the filter-top cover was placed on the cage. The mice were allowed to explore the cage for 30 min. Water and food were withheld during the experiment. Scoring was conducted by weighing the remaining unshredded nestle and dividing this weight by the starting weight to calculate the percentage of nestlets shredded.[29]

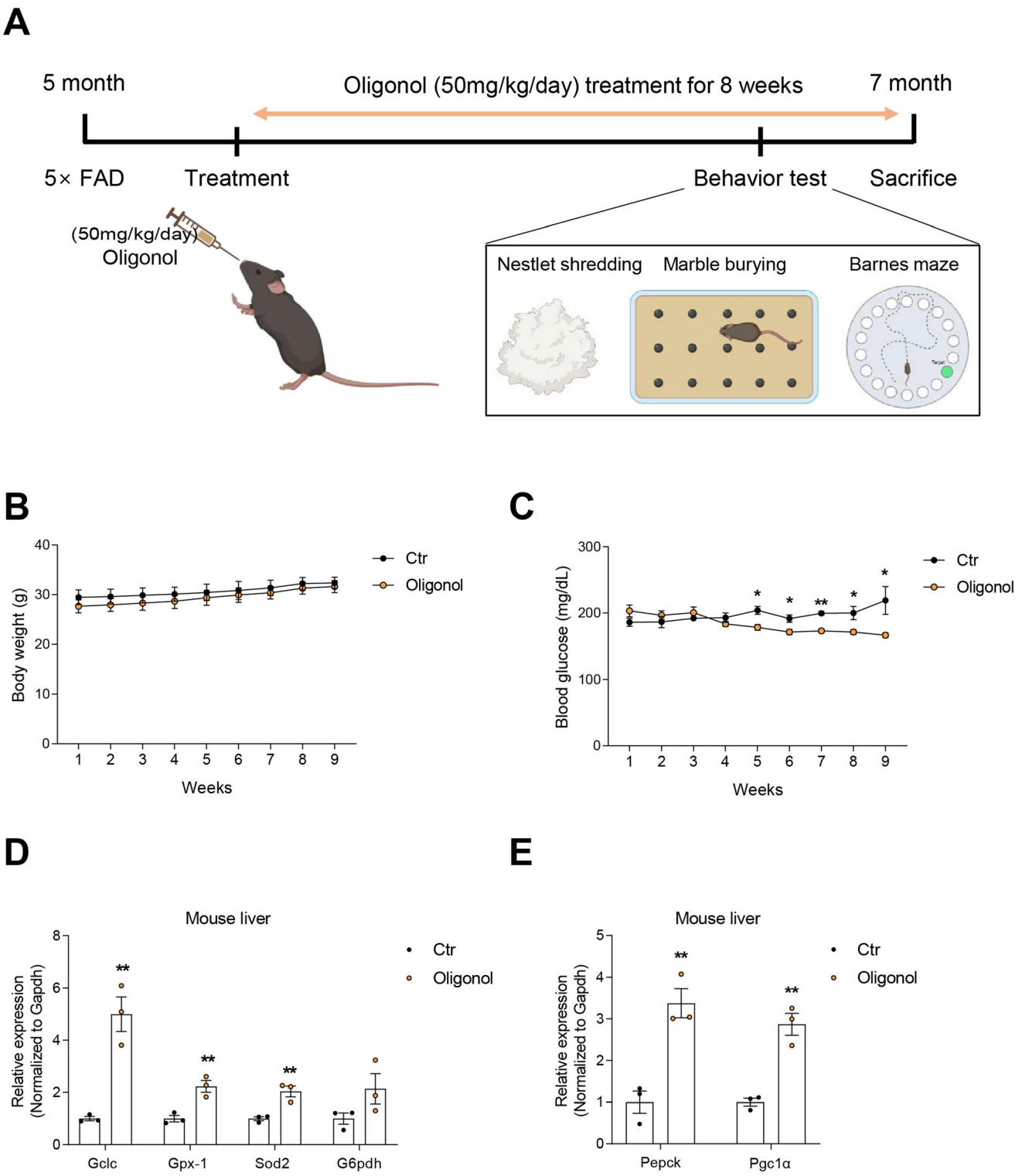

Fig. 1 Metabolic alterations and liver function in oligonol-treated 5 × FAD mice. (A) Schematic of the experimental plan. (B) Body weight measurements of control and oligonol-treated 5 × FAD mice. (C) Blood glucose measurements of control and oligonol-treated mice. (D) The expression level of antioxidant-related genes (*Gclc, Gpx-1, Sod2, and G6pdh*) in control and oligonol-treated mice liver tissues, depicted as the mean ± S.E.M (n = 3). (E) The expression level of gluconeogenesis-related genes (*Pepck* and *Pgc1α*) in control and oligonol-treated mice liver tissues, depicted as the mean ± S.E.M (n = 3). Statistical significance was determined using an unpaired two-tailed t-test with Welch's correction. *$p < 0.05$, **$p < 0.01$.

2.5. Quantitative real-time polymerase chain reaction (RT-PCR)

Total RNA was extracted using TRIzol reagent (Ambicon) according to the manufacturer's protocol. Total RNA from the liver, cortex, and hippocampus of 5 × FAD mice was converted to complementary DNA (cDNA) using random hexamers (Thermo Fisher Scientific) and RevertAid reverse transcriptases (Thermo Fisher Scientific). mRNA expression was measured by quantitative RT-PCR presented using the comparative CT method using the Power SYBR Green PCR master mix (Applied Biosystems) and the Step One Plus PCR system (Applied Biosystems). mRNA expression was normalized to the *Gapdh* primer set. The primer sequences of the mRNAs are listed in Table 1.

2.6. Western blotting

Proteins from the mice cortex and hippocampus were extracted in radioimmunoprecipitation assay buffer (RIPA, Translab) containing 1× phosphatase inhibitors and 1× protease inhibitors for 20 min on ice. Proteins were quantified using a bicinchoninic acid protein assay kit (BCA, Thermo Fisher Scientific) according to the manufacturer's protocol. Proteins (20 g) were loaded on a 10%–12% SDS-PAGE gel, and proteins were transferred onto a polyvinylidene fluoride membrane (PVDF, Millipore) activated by methanol. The membrane was blocked with 5% skim milk (BD Biosciences) or 5% bovine serum albumin (Thermo Fisher Scientific) for 1 h 30 min at room temperature. The membrane was incubated with primary antibodies (1 : 1000 dilution) overnight at 4 °C. The membrane was incubated with horseradish peroxidase (HRP) secondary antibody (Santa Cruz, 1 : 5000 dilution) for 2 h at room temperature. The membrane was detected using an enhanced chemiluminescence (ECL) solution (Thermo Fisher Scientific) and Fusion Solo software (Vilber). Protein expression was quantified using ImageJ software, and all protein expression levels were normalized to the GAPDH expression level. The following primary antibodies: brain-derived neurotrophic factor (BDNF) (Abcam, ab108319), Syp (Millipore, MAB368), c-Fos (Santa Cruz, sc-166940), glial fibrillary acidic protein (GFAP) (Santa Cruz, sc-33673), SR-2A (Santa Cruz, sc-166775), and GAPDH (Santa Cruz, sc-32233).

2.7. Detection of mouse cytokines and adipokines

A cytokine and adipokine array (R&D Systems, ARY006, and ARY013, USA) was performed according to the manufacturer's instructions using 5 × FAD mice. Blood samples of 5 × FAD mice were clotted at room temperature for 15 min and then centrifuged at 10 000 rpm for 10 min to collect plasma. Subsequently, the plasma was diluted and incubated in a blocking solution containing the antibody detection cocktail for 1 h at room temperature, followed by incubating the membranes for cytokine and adipokine detection overnight at 4 °C. After incubating the membranes in streptavidin–horseradish peroxidase solution for 30 min at room temperature, the dot blots were visualized using an ECL solution and Fusion Solo software.

2.8. Transcriptome analysis of RNA sequencing data

Total RNA from the cerebral hippocampus in three 5 × FAD mice models and three oligonol treated 5 × FAD mice models was extracted using TRIzol reagent (Thermo Fisher, MA, USA), and RNA integrity was verified using the Agilent 2100 BioAnalyzer (Agilent, CA, USA). The sequencing reads for each sample were mapped to the reference genome (Mus musculus GRCm39) by Kallisto (v0.46.1).[30] The aligned results were applied to edgeR package[31] to select differentially expressed genes.

2.9. Functional analysis of significantly changed genes

To select genes with significant changes in their expression in the oligonol-treated 5 × FAD group, we first selected transcripts with significantly different expression in the oligonol-treated 5 × FAD mouse data and the corresponding control group data. For this purpose, 577 genes with significant expression changes based on *p*-values 0.05 in the oligonol-treated 5 × FAD groups were selected. We distinguished genes in the volcano plots in Fig. 5A with genes based on *p*-values < 0.05. Statistically, among the genes with *p*-values < 0.05, the

Table 1 RT-PCR Primer lists

Mouse		
Name	Forward sequence	Reverse sequence
Gclc	GTTATGGCTTTGAGTGCTGCAT	ATCACTCCCCAGCGACAATC
Gpx-1	CCAGGAGAATGGCAAGAATGA	TCTCACCATTCACTTCGCACTT
Sod2	TCTCACCATTCACTTCGCACTT	GGTGGCGTTGAGATTGTTCA
G6pdh	CTGGAACCGCATCATCGTGGAG	CCTGATGATCCCAAATTCATCAAAATAG
Pepck	AACTGTTGGCTGGCTCTC	GAACCTGGCGTTGAATGC
Pgc1α	TATGGAGTGACATAGAGTGTGCT	CCACTTCAATCCACCCAGAAAG
Fos	CTGTCCGTCTCTAGTGCCAAC	CCTCCTGACACGGTCTTCAC
Psd95	GGTAACTCAGGTCTGGGCTTC	CACTGCAGCTGAATGGGTCA
Syp	ACATGCAAGGAACTGAGGGA	CCAGGTTCAGGAAGCCAAAC
Cyp2e1	CTTTGCAGGAACAGAGACCA	ATGCACTACAGCGTCCATGA
Cyp4a10	CAACTTGCCCATGATCACACA	CATCCTGCAGCTGATCCTTTC
Gapdh	AATGTGTCCGTCGTGGATCT	AGACAACCTGGTCCTCAGTG

expression values of 328 genes were increased and those of 249 genes were decreased after oligonol treatment in 5 × FAD mice. Among the genes with a p-value < 0.05, we selected 20 increased and 20 decreased genes in the order of fold change. For Gene Ontology (GO) analysis and Kyoto Encyclopedia of Genes and Genomes (KEGG) analysis using the Molecular Signatures Database,[32] we selected 577 genes with p-values < 0.05 in the oligonol-treated 5 × FAD mouse model. The STRING (**https://string-db.org**) software program was used to screen interaction networks of the top 200 genes in order of decreasing p-values among genes with p-values <0.05. We selected only the networks with a minimum of two nodes.

2.10. Statistical analysis

All data are presented as the group mean ± S.E.M. Statistical analysis was performed using an unpaired two-tailed t-test with Welch's correction in GraphPad Prism 8 (GraphPad Software Inc., USA). Data were considered significant at $^{*}p < 0.05$, $^{**}p < 0.01$, and $^{***}p < 0.005$ in the statistical analysis.

3. Results

3.1. Oligonol treatment improved glucose metabolism and increased antioxidant gene expression in the livers of 5 × FAD mice

Oral administration of oligonol (50 mg kg^{-1} day^{-1}) was administered to 5 × FAD mice at 5 months of age for 2 months (Fig. 1A) and the body weight and blood glucose level were checked (Fig. 1A). The body weights of both oligonol-treated and control 5 × FAD mice similarly increased over the 2-month period (Fig. 1B). The blood glucose levels in the oligonol-treated 5 × FAD mice gradually decreased from 4 weeks compared to those in the control 5 × FAD mice (Fig. 1C). The mRNA levels of antioxidant-related genes, such as glutamate-cysteine ligase catalytic (*Gclc*), glutathione peroxidase 1 (*Gpx1*), superoxide dismutase 2 (*Sod2*), and glucose 6-phosphate dehydrogenase (*G6pdh*), were significantly increased in the liver tissues of oligonol-treated 5 × FAD mice compared to the control 5 × FAD mice (Fig. 1D). Additionally, the mRNA levels of gluconeogenesis-related genes, such as phosphoenolpyruvate carboxykinase (*Pepck*) and peroxisome proliferator-activated receptor-c coactivator-1a (*Pgc1α*), were dramatically increased in the liver tissues of oligonol-treated 5 × FAD mice compared to control 5 × FAD mice (Fig. 1E).

3.2. Oligonol treatment improved anxiety behavior and cognitive function in 5 × FAD mice

We conducted the MBT and NST to investigate the anxiety behavior, and the Barnes maze to examine the cognition in 5 × FAD mice after oral administration of oligonol (Fig. 2). The marble burying score, considered as the number of buried marbles, was significantly decreased in the oligonol-treated 5 × FAD mice (Fig. 2A). The nestle shredding score, considered as the weight of shredded material (g), was significantly reduced in oligonol-treated 5 × FAD mice (Fig. 2B). Fig. 2A and B show the suppressed anxiety in 5 × FAD mice as a result of oligonol treatment. We conducted the Barnes maze test to investigate the cognitive function in oligonol-treated 5 × FAD mice (Fig. 2D–L). Fig. 2C shows the quadrant region and target hole in the Barnes maze (Fig. 2C), while Fig. 2D and E show the percentage of each quadrant region visit on days 1 and 7 (Fig. 2D and E). Oligonol-treated 5 × FAD mice approached the C1 quadrant region containing the escape hole more frequently than the control 5 × FAD mice (Fig. 2D and E). Oligonol-treated 5 × FAD mice also showed a reduced total distance (Fig. 2F), immobility time (Fig. 2G), and velocity (Fig. 2H) to find escape holes on day 7. Additionally, oligonol-treated 5 × FAD mice demonstrated a reduced number of visits (Fig. 2I), decreased latency (Fig. 2J), reduced attempts in the target escape hole (Fig. 2K), and reduced total errors (Fig. 2L) in the fine target escape hole on day 7. These Barnes maze scores indicate that oligonol treatment improves cognitive function in 5 × FAD mice.

3.3. Oligonol treatment alters the secretion of inflammatory cytokines and adipokines in the blood plasma of 5 × FAD mice

We detected various cytokines and adipokines in the blood plasma of 5 × FAD mice after oral administration of oligonol using cytokine and adipokine array kits (Fig. 3). The results revealed increased expression of cytokines, such as B lymphocyte chemoattractant (Blc) and tissue inhibitor of metalloproteinase-1 (TIMP-1), and reduced expression of interferon gamma (IFN-γ) and the chemokine ligand C–X–C motif chemokine ligand 12 (CXCL12) in the blood plasma of oligonol-treated 5 × FAD mice (Fig. 3A). We also found increased levels of adipokines, such as insulin-like growth factor 2 (IGF-2) and fibroblast growth factor 21 (FGF21), and dramatically reduced levels of oncostatin M (OSM) in the blood plasma of oligonol-treated 5 × FAD mice (Fig. 3B). These data indicate that oligonol influences the levels of cytokines and adipokines in the blood of 5 × FAD mice.

3.4. Oligonol treatment reduces the expression of reactive oxygen species (ROS)-generating genes and increases the expression of neuronal function-related genes and serotonin receptors in the brains of 5 × FAD mice

We next investigated the mRNA levels of neuronal function-related genes (*c-FOS*, *PSD95*, and *SYP*) and ROS generating genes (*Cyp2e1* and *Cyp4a10*) in the cortex, hippocampus, and striatum regions of the brains of 5 × FAD mice oral administration (Fig. 4). We detected increased mRNA levels of *PSD95* and *SYP* genes, as synaptic function-related markers, and c-Fos, as neuronal functional markers, in the mouse cortex (Fig. 4A), hippocampus (Fig. 4C), and striatum (Fig. 4E) of 5 × FAD mice after oligonol treatment (Fig. 4A, C, and E). We also observed reduced mRNA levels of *Cyp2e1* and *Cyp4a10* genes, as genes related to ROS generation, in the mouse cortex (Fig. 4B), hippocampus (Fig. 4D), and striatum (Fig. 4F) of 5 × FAD mice after oligonol treatment. Furthermore, we confirmed the protein levels of m-BDNF, Syp, c-Fos, and GFAP in the mouse cortex, hippocampus, and striatum of 5 × FAD mice

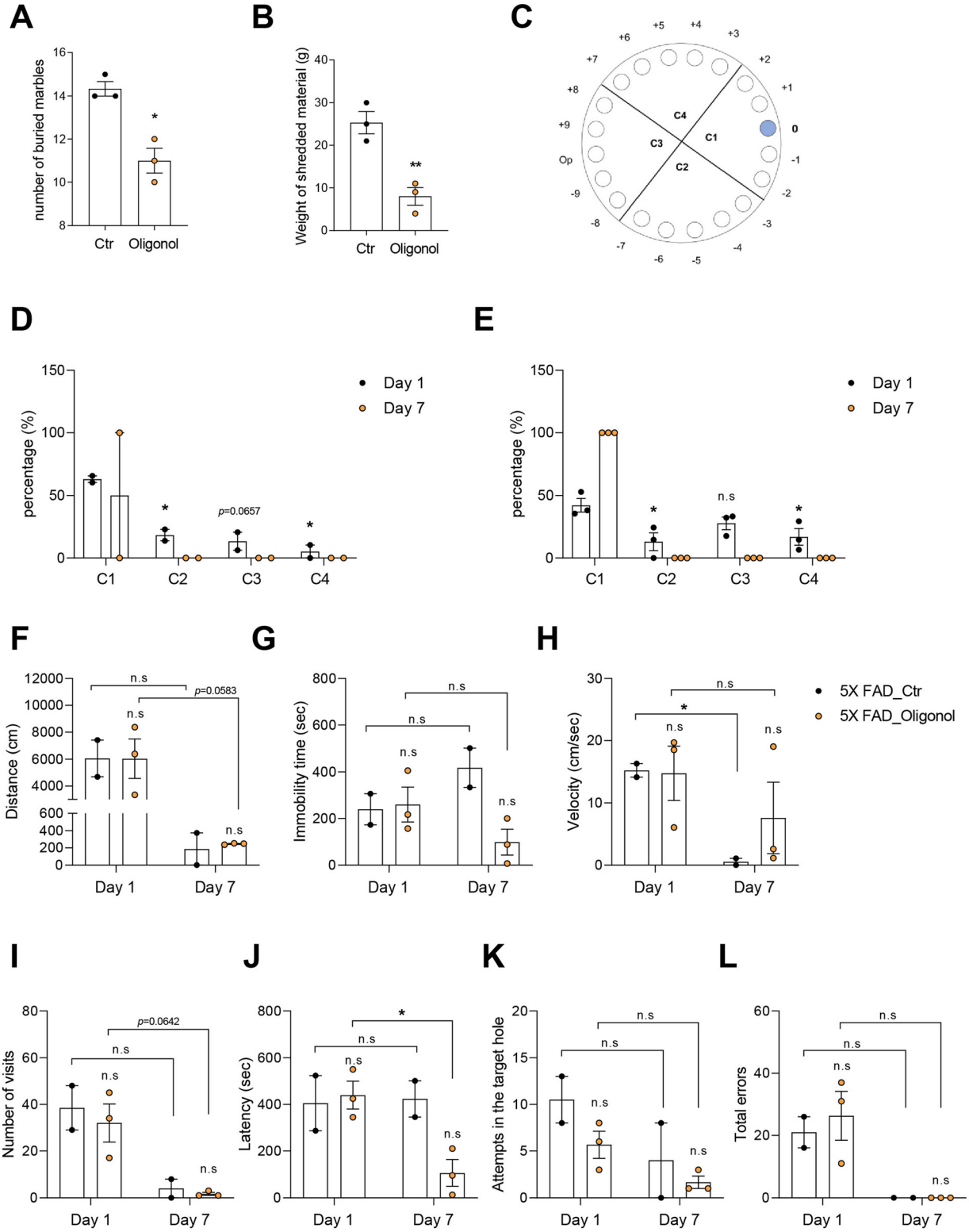

Fig. 2 Behavioral tests in oligonol-treated 5 × FAD mice. (A) Measurement of the number of buried marbles in control and oligonol treated 5 × FAD mice. (B) Measurement of nestlet shredding activity, represented as grams of shredded materials after the test. (C) Schematic of the Barnes maze apparatus. (D) Percentage of latency per quadrant on days 1 and 7 in the control group. (E) Percentage of latency per quadrant on days 1 and 7 in the oligonol-treated group. (F) Changes in the total movement (cm), (G) immobility time (s), and (H) velocity (cm s^{-1}), for control and oligonol mice. (I) Number of visits to each hole on days 1 and 7. (J) Measurement of escape latency (s) to the target hole on days 1 and 7. (K) Number of trials to the target hole on days 1 and 7. (L) Number of trials to non-target holes on days 1 and 7. Statistical significance was determined using an unpaired two-tailed *t*-test with Welch's correction. ns: not significant, $*p < 0.05$, $**p < 0.01$.

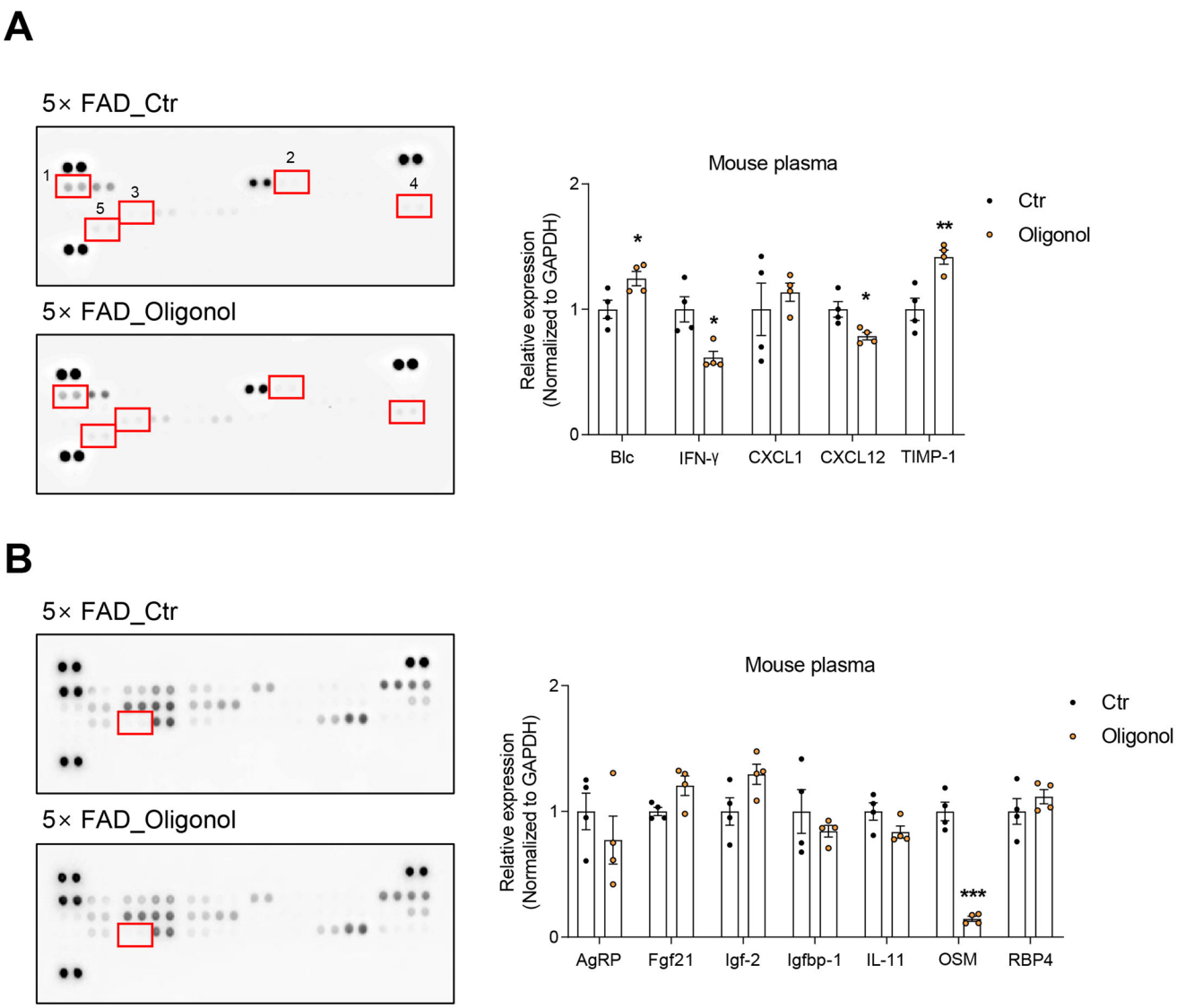

Fig. 3 Cytokine and adipokine arrays of the plasma of oligonol-treated 5 × FAD mice. (A) Immunoblot analysis of cytokine and chemokine levels in control and oligonol-treated mouse plasma. The red box on the membrane represents the spots of Blc, IFN-γ, CXCL1, CXCL12, and TIMP-1 in the indicated numerical order. (B) Immunoblot analysis of adipokine levels in control and oligonol-treated mouse plasma. The red box on the membrane represents the OSM spot. The statistical analysis of differential expression levels was performed using an unpaired two-tailed *t*-test with Welch's correction. ns: not significant, $*p < 0.05$, $**p < 0.01$, $***p < 0.005$.

following oligonol treatment (ESI Fig. 2†). We found an increased protein level pattern of GFAP, considered to indicate glial activation in the cortex (ESI Fig. 2A†), an increased protein level of c-Fos, considered to indicate neuronal activation in the hippocampus (ESI Fig. 2B†), and an increased protein level of c-Fos and SYP, considered to indicate neuronal activation and synaptic function in the striatum (ESI Fig. 2C†). Although these ESI Fig. 2† data are not significant, they reveal an increased pattern of proteins associated with neuronal function. Furthermore, we detected increased protein levels of serotonin receptors in the striatum region of 5 × FAD mice following oligonol treatment (Fig. 4G). Collectively, these findings show that oligonol treatment inhibits ROS generation and enhances synaptic plasticity, neuronal function, glial activation, and the expression of serotonin receptors in the brains of 5 × FAD mice.

3.5. Transcriptome analysis of the hippocampus in oligonol-treated 5 × FAD mice

For transcriptome analysis of the hippocampus in oligonol-treated 5 × FAD mice, we conducted RNA sequencing of the total RNA in the hippocampus of three oligonol-treated 5 × FAD mice and three corresponding control 5 × FAD mice. First, we checked that the grouping between 5 × FAD group genes and oligonol treatment group genes was well performed (Fig. 5A). In the RNA sequencing data, the genes with exceptionally high expression levels and genes showing statistically significant changes in the oligonol-treated 5 × FAD group are

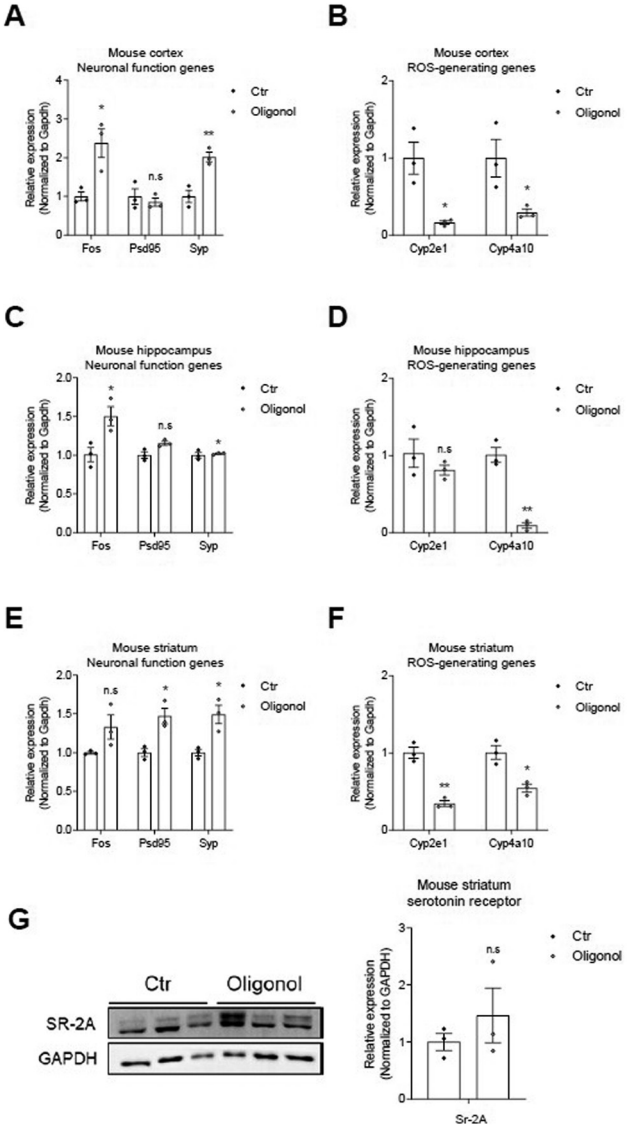

Fig. 4 mRNA and protein levels in the brain tissues of oligonol-treated 5 × FAD mice. (A) The expression level of neuronal function related genes (*c-Fos, Psd95,* and *Syp*) in control and oligonol-treated mice cortex tissues, described as the mean ± S.E.M (n = 3). (B) The expression level of reactive oxygen species (ROS)-generating related genes (*Cyp2e1* and *Cyp4a10*) in control and oligonol-treated mice cortex tissues, described as the mean ± S.E.M (n = 3). (C) The expression level of neuronal function-related genes (*c-Fos, Psd95,* and *Syp*) in control and oligonol-treated mice hippocampus tissues, depicted as the mean ± S.E.M (n = 3). (D) The expression level of genes related to ROS generation (*Cyp2e1* and *Cyp4a10*) in control and oligonol-treated mice hippocampus tissues, depicted as the mean ± S.E.M (n = 3). (E) The expression level of neuronal function related genes (*c-Fos, Psd95* and *Syp*) in control and oligonol-treated mice striatum tissues, described as the mean ± S.E.M (n = 3). (F) The expression level of genes related to ROS generation (*Cyp2e1* and *Cyp4a10*) in control and oligonol-treated mice striatum tissue, described as the mean ± S.E.M (n = 3). (G) The expression level of serotonin receptor SR-2A protein in control and oligonol-treated mice striatum tissues, depicted as the mean ± S.E.M (n = 3). The statistical analysis of differential expression levels was performed using an unpaired two-tailed t-test with Welch's correction. ns: not significant, *p < 0.05, **p < 0.01.

shown in the volcano plot graph (Fig. 5B). Analysis of the hippocampus of an oligonol-treated 5 × FAD mouse revealed 328 genes with significantly increased expression and 249 genes with significantly decreased expression with a p-value of 0.05. As depicted in the volcano plot, the expression of *Gm15772*, *Slc6a3*, tryptophan hydroxylase 2 (*Tph2*), small nucleolar RNA, C/D Box 49B (*Snord49b*), *Gm15461*, spindle and centriole associated protein 1 (*Spice1*), Gm20618, growth hormone (*Gh*), and s100 calcium binding protein A7A (*S100a7a*) was significantly distinguished in the oligonol-treated 5 × FAD mouse hippocampus (Fig. 5B). Next, we identified fold changes in 20 genes with p-values < 0.05 in transcriptome data (Fig. 5C). Our results showed that fold-change-increased genes related to neuropathology were dermokine (*Dmkn*), cadmium-12 (*Cdh12*), stabilizer of axonemal microtubules 2 (*Saxo2*), apolipoprotein L domain-containing 1 (*Apold1*), POC1 centriolar protein A (*Poc1a*), anoctamin 3 (*Ano3*), potassium voltage-gated channel subfamily H member 7 (*Kcnh7*), membrane metallopentase (*Mme*), ATPase plasma membrane Ca^{2+} transporting 1 (*Atp2b1*), cannabinoid receptor 1 (*Cnr1*), X-ray repair cross complementing 4 (*Xrcc4*), calcium/calmodulin dependent protein kinase IV (*Camk4*), doublecortin-like kinase 3 (*Dclk3*), phosphodiesterase 10A (*Pde10a*), regulator of G protein signaling 4 (*Rgs4*), cyclin-dependent kinase-like 5 (*Cdkl5*), homer scaffold protein 1 (*Homer1*), HIVEP zinc finger 2 (*Hivep2*), leucine rich repeat-containing 8 VRAC subunit B (*Lrrc8b*), and synaptotagmin 1 (*Syt1*) genes in fold change order (Fig. 5C). We also checked the fold changes in 20 decreased genes with p-values < 0.05 in transcriptome data (Fig. 5D). Our results showed that the genes associated with decreased fold change in neuropathology were RalA binding protein 1 (*Ralbp1*), chitinase 3-like 1 (*Chil1*), fumarylacetoacetate hydrolase (*Fah*), solute carrier family 38 member 10 (Slc38a10), peroxisome proliferator activated receptor delta (*Ppard*), progestin and AdipoQ receptor family member 3 (*Paqr3*), F-Box protein 7 (*Fbxo7*), phospholipid phosphatase 2 (*Phlpp2*), myosin IXB (*Myo9b*), CCR4-NOT transcription complex subunit 3 (*Cnot3*), ATP-binding cassette A7 (*Abca7*), AXL receptor tyrosine kinase (*Axl*), cytoplasmic endogenous regulator of oxidative phosphorylation 1 (*Cerox1*), abhydrolase domain-containing 4, *N*-acyl phospholipase B (*Abhd4*), pleckstrin homology and RUN domain containing M2 (*Plekhm2*), strawberry notch homolog 2 (*Sbno2*), regulatory factor X associated ankyrin-containing protein (Rfxank), deoxythymidylate kinase (*Dtymk*), leucine rich repeat-containing 45 (*Lrrc45*), and small nuclear ribonucleoprotein U1 subunit 70 (*Snrnp70*) genes in fold change order (Fig. 5D). ESI Table 1† shows the 577 genes with p-value 0.05 or less genes (ESI Table 1†).

Additionally, to identify the cellular pathways associated with genes significantly changed in the hippocampus of the oligonol-treated 5 × FAD mice, we performed GO analysis in The Molecular Signatures Database (MSigDB) with 577 genes with p-values < 0.05 (Fig. 6A). GO analysis showed that the most significantly enriched terms were anatomical structure morphogenesis, synapse organization, Ras protein signal transduction, positive regulation of phosphorylation, positive

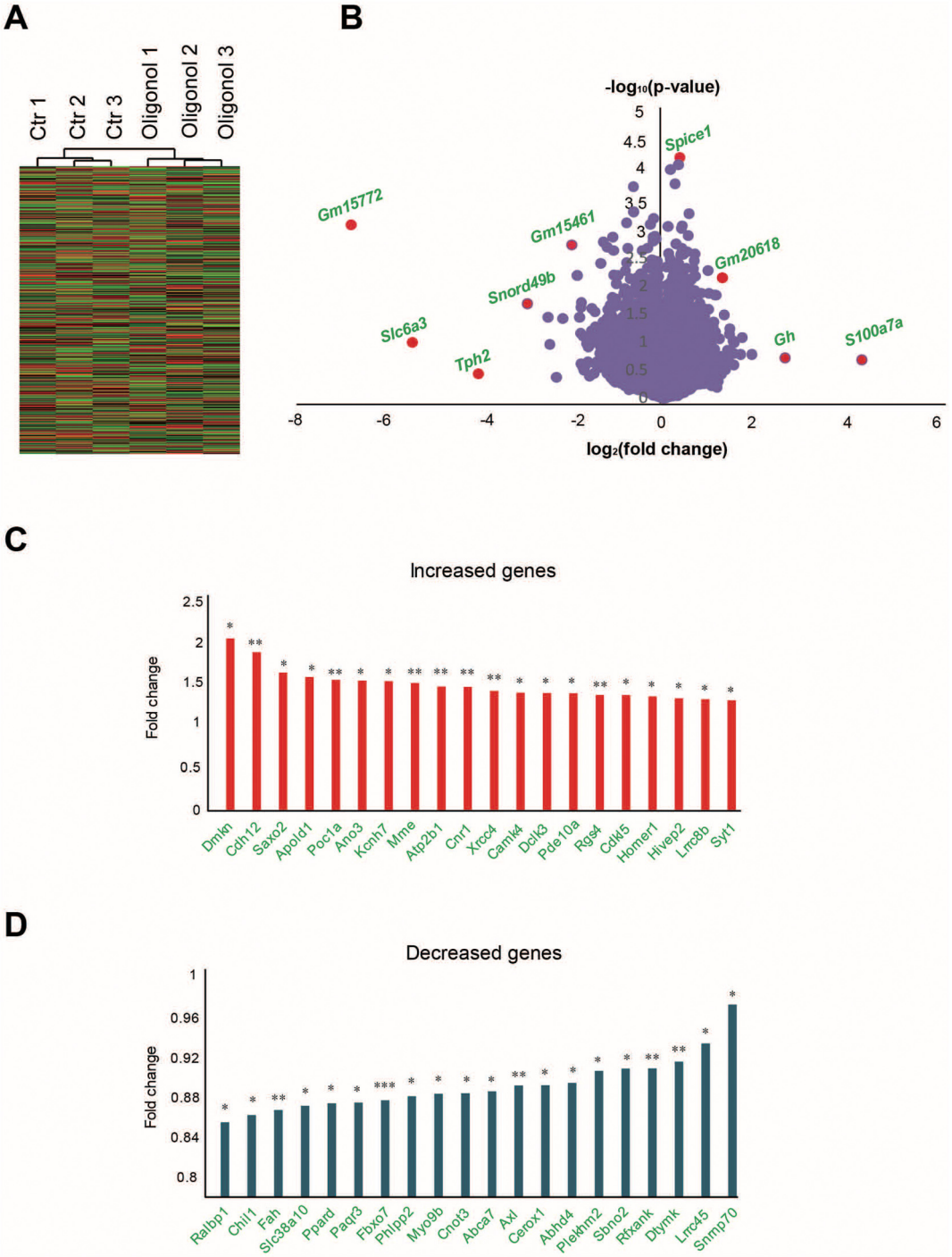

Fig. 5 Analysis of transcriptomic data from the brain hippocampus of oligonol-treated 5 × FAD mouse models. (A) The expression profiles of the oligonol-treated 5 × FAD group hippocampus are presented as heat maps after RNA sequencing. (B) Volcano plots of the oligonol-treated 5 × FAD group hippocampus. The *X*-axis represents the log2-transformed fold change, and the *Y*-axis represents the $-\log_{10}$ (*p*-value) value. All red dots depict significantly changed genes. (C) The 20 increased genes with a significant expression change in oligonol-treated 5 × FAD models. The graphs are depicted for increased genes in fold change order in the oligonol-treated 5 × FAD mouse hippocampus. (D) The 20 decreased genes with a significant expression change in oligonol-treated 5 × FAD mice. The graphs depict increased genes in fold change order in the oligonol-treated 5 × FAD mouse hippocampus. The statistical analysis of differential expression levels was performed using an unpaired two-tailed *t*-test with Welch's correction. ns: not significant, $*p < 0.05$, $**p < 0.01$, $***p < 0.005$.

regulation of transferase activity, regulation of endocytosis, calcium ion homeostasis, regulation of synaptic plasticity, neuron development, cellular component biogenesis, organophosphate metabolic process, cell part morphogenesis, divalent inorganic cation homeostasis, regulation of protein modification process, and regulation of transferase activity (Fig. 6A).

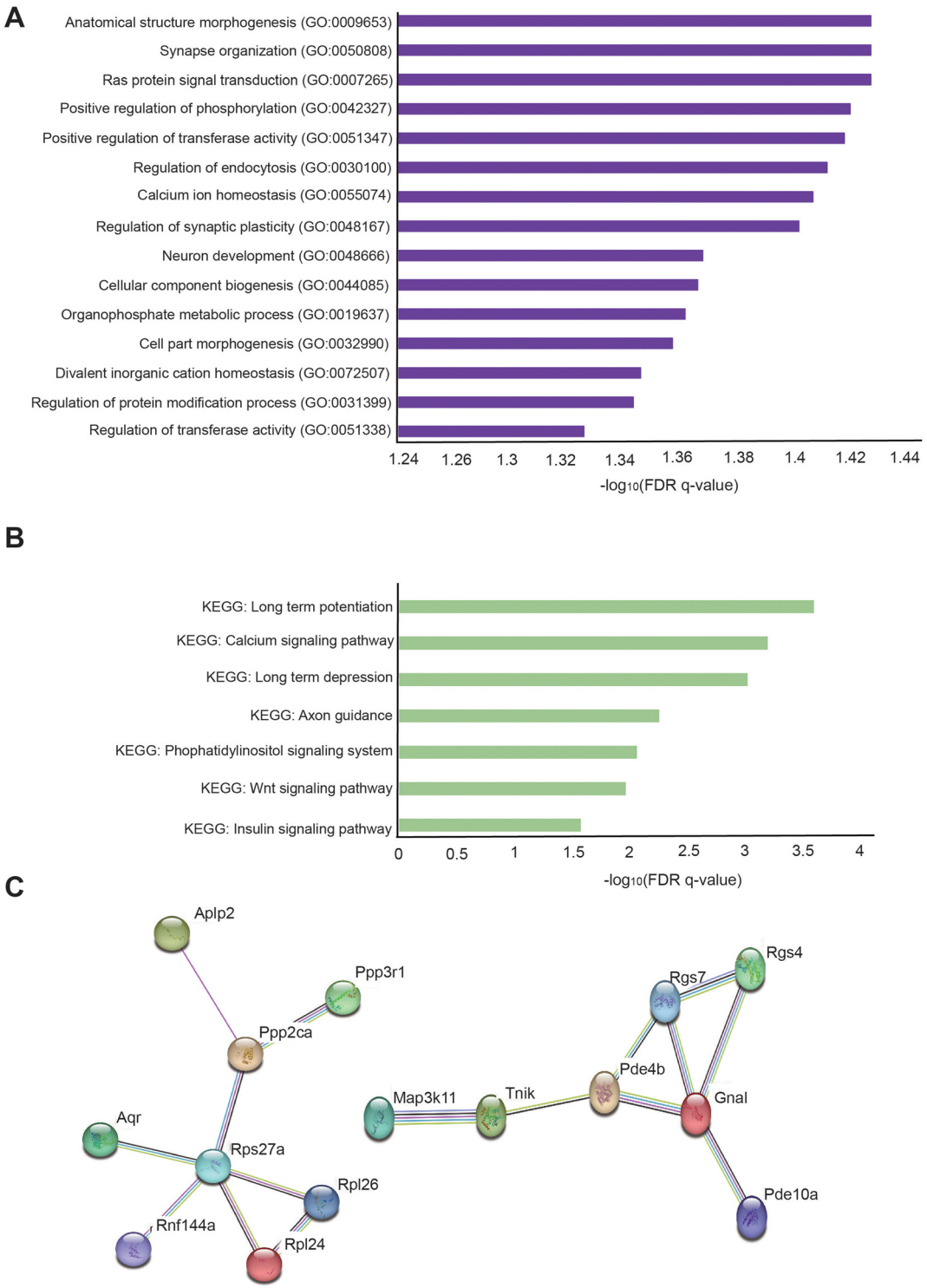

Fig. 6 Functional analysis of changed genes in the oligonol-treated 5 × FAD mouse hippocampus. (A) Gene ontology (GO) analysis for changed genes in the oligonol-treated 5 × FAD mouse hippocampus. The top 15 GO terms based on the false discovery rate (FDR) *q*-value are shown. (B) Kyoto encyclopedia of genes and genomes (KEGG) analysis for changed genes in the oligonol-treated 5 × FAD mouse hippocampus. The top seven KEGG terms based on the false discovery rate (FDR) *q*-value are shown. (C) Analysis of the protein interaction network for changed genes in oligonol-treated 5 × FAD groups using the STRING database.

We also performed KEGG pathway analysis in MSigDB with 577 genes with *p*-values 0.05 (Fig. 6B). KEGG analysis showed that the most significant terms were long-term potentiation, calcium signaling pathway, long-term depression, axon guidance, phosphatidylinositol signaling system, Wnt signaling pathway, and insulin signaling pathway (Fig. 6B). Next, to

analyze the protein networks affected in the oligonol-treated 5 × FAD mouse hippocampus, we selected 200 genes in order of low *p*-values among genes with *p*-values < 0.05. We then analyzed the STRING network analysis database using selected genes[33] (Fig. 6C). The protein interaction network obtained from the STRING database for the genes that were changed in the oligonol-treated 5 × FAD group is shown in Fig. 6C. Interestingly, the network containing the APLP2 protein, related to the amyloid precursor protein, the RGS7 protein, related to the GTPase activating protein in the brain, the PDE4B and RGS4 proteins, related to schizophrenia, and the TNIK protein, related to postsynaptic density of glutamatergic synapse and neuropsychiatric disorders were selected after STRING analysis (Fig. 6C).

4. Discussion

Here, we investigated the role of oligonol in metabolic condition and cognitive function in 5 × FAD mice, which together with 3TG mice, is a widely used AD mouse model.[34,35] In particular, the 5 × FAD mouse is an AD model that rapidly develops severe amyloid pathologies within 2–4 months after birth.[35] During the oral administration of oligonol to 5 × FAD mice, we checked the body weight and blood glucose levels every week until the day of sacrifice. We observed a reduction in blood glucose levels in the oligonol-treated 5 × FAD mice compared to control mice. A previous study mentioned that oligonol improved insulin sensitivity and glucose uptake.[36] We previously confirmed the positive regulatory role of oligonol in glucose metabolism in AD mice. We have also detected increased mRNA levels of antioxidant-related genes, such as *Gclc*,[37] *Gpx1*,[38] *Sod2*,[39] and *G6pdh*,[40] and nuclear factor erythroid-2-related factor 2 (*Nrf2*)[41] in the livers of 5 × FAD mice (Fig. 1). Increased expression of these genes indicates that oligonol treatment causes an increased antioxidant response in the liver and reduced liver damage in AD mice.[42] In addition, the increased levels of *Pepck* and *Pgc1α* genes observed in our study are associated with gluconeogenesis through the activation of PI3K/AKT signaling.[43,44] *PGC-1α* regulates the mitochondrial catabolic capacity of the cell and boosts the expression of antioxidant enzymes against damage conditions.[45–47] These findings indicate that oligonol promotes the antioxidant response and plays a cellular protective role in the livers of AD mice.

In this study, we performed three behavior tests (Barnes maze test, BMT, and NST). The Barnes maze test, as one of the major behavior tests, is used to assess spatial memory and learning function more accurately than previous tests such as the Morris water maze.[48–52] Several studies have used the Barnes maze to investigate learning and memory deficits in AD model mice.[53,54] The results of the Barnes maze test suggest that oligonol enhances spatial memory in the AD brain. MBT is used to investigate anxiolytic behavior[55] and obsessive–compulsive behavior.[56] Wild-type mice usually *dig* in the ground to search for food, bury harmful things, and create safe nurseries for their babies.[28] Some studies have attempted to investigate the behavioral and psychological symptoms of dementia, such as anxiety, in AD mouse models using the MBT.[34,57–59]Considering the MBT scores observed in our study, oligonol may alleviate anxiety-like psychiatric problems in the AD brain. Additionally, the NST is a behavior test to assess psychiatric diseases such as anxiety, compulsive-like behaviors, distress, and pain.[60–62] Some studies have identified brain functional deficits and brain damage using the NST.[63,64] Our results suggest that oligonol improves anxiety, compulsive-like behavior, and distress in the AD brain. The data shown in Fig. 4G confirm the increased expression of the serotonin receptor SR-2A in the striatum. The serotonin receptor 5-HT 2a is commonly expressed on neurons and glia in the cortex, nucleus accumbens, claustrum, olfactory bulb, limbic system, striatum including the amygdala, and basal ganglia.[65,66] Several studies have mentioned that reduced serotonin 5-HT 2a receptors are associated with object memory loss, spatial memory loss,[67,68] and reduced long term memory[69] in AD. Other studies have reported that reductions in serotonin 5-HT 2a receptors lead to impaired fear memory, mental disorders, depression and anxiety.[70–73] Serotonin 5-HT 2a receptors colocalize with PSD-95 protein[74] and influence dendritic spine maturation and synapse stabilization.[75] Serotonin 5-HT 2a receptor signaling also induces intercellular signaling pathway activation, including ERK and tyrosine kinase signaling in neurons.[76] Accordingly, our results indicate that oligonol enhances the serotonergic system in the brains of 5 × FAD mice and improves anxiety, spatial memory, and depression in the AD brain.

Subsequently, we detected the cytokine and adipokine levels in the blood plasma of 5 × FAD mice. Our data revealed that oligonol treatment increased the levels of Blc (CXCL13), related to T cell activity and THE immune response,[77] and I-TAC, a chemokine that regulates the activity of T cells,[78] in the blood plasma of 5 × FAD mice. Oligonol treatment also reduced the levels of INF-γ and IL-27, which serve to heighten the immune and inflammatory responses by T cell polarization, T-cell proliferation, and T cell activation[79,80] in the plasma of 5 × FAD mice. Additionally, the level of oncostatin M, an IL-6 family member that accelerates severe inflammation,[81] was dramatically reduced in the blood plasma of 5 × FAD mice following oral administration of oligonol. In contrast, the levels of IGF-2, an anti-inflammatory regulator and enhancer of neuronal density,[82] and FGF21, an anti-inflammatory regulator,[83] were considerably increased in the plasma of 5 × FAD mice following oral administration of oligonol. Based on the data obtained for cytokines and myokines, we speculate that oligonol treatment suppresses the inflammatory response and contributes to the immune system in AD mice.

Furthermore, we confirmed increased mRNA levels and protein level patterns of synapse-related genes, including *c-Fos, PSD95*, and *SYP*, in the cortex, hippocampus, and striatum of 5 × FAD mice as a result of oligonol treatment. Overall, we hypothesize that oligonol treatment contributes to the expression of neuronal activation and synaptic plasticity in the

brains of 5 × FAD mice. c-Fos, as an index of neuronal activity, has been reported to be associated with several neurological issues, including anxiety, depression, fear memory, and spatial memory.[84–87] PSD95, as a postsynaptic density protein, regulates the localization of various neurotransmitter receptors,[88,89] clustering of ion channels,[90] and synaptic plasticity.[91] SYP, as a presynaptic density protein, regulates neuronal networks and affects cognitive function,[92,93] and depressive like behavior and anxiety.[94] Considering this evidence, we consider that oligonol serves to modulate synapse plasticity and neuronal activity, which is involved in neuropathological issues.

We also observed that the mRNA levels of *Cyp2e1* and *Cyp4a10* genes related to ROS generation in mitochondria[95,96] were decreased in the brain cortex, hippocampus, and striatum of 5 × FAD mice treated with oligonol. This may indicate that oligonol suppresses ROS generation in the cortex, hippocampus, and striatum of the AD brain. Decreased ROS generation in the cortex and hippocampus is linked to enhanced long-term potentiation,[97] improved learning and memory function,[98] reduced neuronal apoptosis,[99] the inhibition of blood–brain barrier (BBB) breakdown,[100] and reduced pain.[101] Increased ROS production in the striatum induces apoptosis,[102] hyperglycemia,[103] Impaired dopamine release and synaptic plasticity.[104] Our data suggest that oligonol can restore dysfunctions caused by ROS production, suggesting that the expression of genes related to ROS generation was reduced by oligonol treatment in the striatum. Our western blot data showed an increased protein level of GFAP in the cortex of 5 × FAD mice after oligonol treatment. Increased GFAP levels are related to astrocyte reactivity,[105] neurogenesis,[106] attenuation of depressive like behavior,[107] and neuronal cell survival[108] through autophagy in the brain.

The volcano graph demonstrates the distinguishing genes of the dopamine transporter *Slc6a3* gene, related to neuropsychiatric diseases,[109,110] *Tph2*, related to serotonergic neuronal cell regulation,[111,112] and *Gh*, related to inflammation.[113] In addition, our transcriptome data showed 20 increased genes, including *Cdh12*, related to the upregulation of neurite growth;[114] *Apold1*, associated with angiogenesis and blood brain permeability;[115,116] *Poc1a*, related to the regulation of neuronal spindle function;[117] *Kcnh7*, associated with the downregulation of schizophrenia;[118] *Atp2b*, related to the protection of γ-aminobutyric acid (GABA)ergic neurons;[119] *Cnr1*, related to mood disorder and dopaminergic neurotransmission;[120,121] *Camp4*, related to the upregulation of memory formation improvement;[122] *Dclk3*, associated with neuroprotective function in the dentate gyrus in hippocampal formation and Huntington's disease;[123] *Pde10a*, related to regulation of the dopamine system in neurons;[124] *Rgs4*, associated with neurotransmitter transmission, psychiatric disorders such as depression and autism, and cognition;[125–127] *Cdkl5*, related to the downregulation of seizure and motor dysfunction;[128] *Homer1*, related to the downregulation of epilepsy, autism, addiction, schizophrenia, and depression;[128] *Hivep2*, related to the regulation of dopaminergic neurons;[129] and *Syt1*, related to the regulation of neurotransmitter release[130] in the 5 × FAD mouse hippocampus after oligonol treatment.

We also found 20 decreased genes, including *Ralbp1*, related to mitochondrial function and decreased neuroinflammation;[131,132] *Slc38a10*, related to the upregulation of cell survival and the homeostasis of neurotransmitters such as GABA, dopamine, serotonin, and glutamate;[133] *Ppard*, associated with the protection of axonal injury and cell growth and the regulation of immune response;[134] *Paqr3*, related to the regulation of energy metabolism, and Golgi apparatus;[135] *Fbxo7*, related to the upregulation of pyramidal neuronal function with Pink1;[136,137] *Myo9b*, related to the maintenance of the dendrite morphology of neurons;[138] *Abca7*, associated with the downregulation of the phagocytosis process in glia, and the process of Alzheimer's disease;[139,140] *Sbno2*, related to the downregulation of interleukin-6 secretion, and the suppression of inflammation;[141,142] and *Snrnp70*, related to the inhibition of amyotrophic lateral sclerosis and motoneuronal degeneration[143,144] in the 5 × FAD mouse hippocampus after oligonol treatment.

Considering our transcriptome analysis data, we found enriched GO terms, including calcium signaling, which is promoted by synaptic activity;[145] the regulation of endocytosis, which modulates the hippocampal synapse strength[146] and neuronal survival;[147] and RAS protein signaling for the regulation of hippocampal neurogenesis and cognition[148] in the 5 × FAD mouse hippocampus after oligonol treatment. We also observed significant KEGG terms such as long-term potentiation, long-term depression which are linked to neurotransmitter secretion, synaptic plasticity, neuronal circuit, learning and memory function;[149–151] axon guidance, which is related to improved hippocampal circuit and synaptogenic activity;[152] Wnt signaling, which is related to hippocampal neurogenesis;[153] and insulin signaling, which can regulate energy homeostasis, cognition, and mood[154,155] in the 5 × FAD mouse hippocampus after oligonol treatment.

Our STRING protein network software data showed the interaction between Ppp2ca, related to neuropsychiatric diseases;[156] Aplp2, associated with amyloid beta peptide processing;[157] and Rps27a, affecting microglia activation.[158] Additionally, Tnik, related to cognition and postsynaptic formation;[159] Rgs7, associated with synaptic plasticity and memory formation;[160] Pde4b, related to the inhibition of memory acquisition;[161] and Pde10a, related to the secretion of dopamine by neurons.[124]

In summary, oral oligonol administration may contribute to the activation of the antioxidant response pathway, reduce ROS generation, modulate glucose metabolism and cytokine and adipokine production, increase glial reactivity, activate synaptic plasticity and neuronal function, and increase serotonin receptor expression in AD. These consequences may lead to stable mood conditions and improved cognitive function in the AD brain. Taken together, our results suggest that oligonol has therapeutic potential to ameliorate liver function and metabolic function and attenuate neuropathological and neuropsychiatric issues such as anxiety and cognitive decline in AD.

Consent for publication

All authors have reviewed the manuscript and provided consent for publication.

Ethics approval and consent to participate

All animal procedures were performed in accordance with protocols approved by the recommendations of the 96 guidance for animal experiments established by the Animal Ethics Committee at Chonnam National University (CNU). The Animal Ethics Committee approved the protocol at the CNU.

Abbreviations

AD	Alzheimer's disease
Aβ	Amyloid beta
SAMP8	Senescence-accelerated prone mice
MBT	Marble burying test
NST	Nestlet shredding behavior test
cDNA	Complementary DNA
Gclc	Glutamate-cysteine ligase catalytic
Gpx1	Glutathione peroxidase 1
Sod2	Superoxide dismutase 2
G6pdh	Glucose 6-phosphate dehydrogenase
Pepck	Phosphoenolpyruvate carboxykinase
Pgc1α	Peroxisome proliferator-activated receptor-c coactivator-1a
Blc	B lymphocyte chemoattractant
TIMP-1	Metalloproteinase-1
IFN-γ	Interferon gamma
CXCL12	Chemokine ligand C–X–C motif chemokine ligand 12
IGF-2	Insulin-like growth factor 2
FGF21	Fibroblast growth factor 21
OSM	Oncostatin M
ROS	Reactive oxygen species
Tph2	Tryptophan hydroxylase 2
Snord49b	Small Nucleolar RNA: C/D Box 49B
Spice1	Spindle and centriole associated protein 1
Gh	*Growth hormone*
S100a7a	s100 calcium binding protein A7A
Dmkn	Dermokine
Cdh12	Cadherin-12
Saxo2	Stabilizer of axonemal microtubules 2
Apold1	Apolipoprotein L domain-containing 1
Poc1a	POC1 centriolar protein A
Ano3	Anoctamin 3
Kcnh7	Potassium voltage-gated channel subfamily H member 7
Mme	Membrane metalloendopeptidase
Atp2b1	ATPase plasma membrane Ca^{2+} Transporting 1
Cnr1	Cannabinoid receptor 1
Xrcc4	X-ray repair cross complementing 4
Camk4	Calcium/calmodulin dependent protein kinase IV
Dclk3	Doublecortin-like kinase 3
Pde10a	Phosphodiesterase 10A
Rgs4	Regulator of G protein signaling 4
Cdkl5	Cyclin-dependent kinase-like 5
Homer1	Homer scaffold protein 1
Hivep2	HIVEP zinc finger 2
Lrrc8b	Leucine rich repeat-containing 8 VRAC subunit B
Syt1	Synaptotagmin 1
Ralbp1	RalA binding protein 1
Chil1	Chitinase 3-like 1
Fah	Fumarylacetoacetate hydrolase
Slc38a10	Solute carrier family 38 member 10
Ppard	Peroxisome proliferator activated receptor delta
Paqr3	Progestin and adipoQ receptor family member 3
Fbxo7	F-box protein 7
Phlpp2	Phospholipid phosphatase 2
Myo9b	Myosin IXB
Cnot3	CCR4-NOT transcription complex subunit 3
Abca7	ATP-binding cassette A7
Axl	AXL Receptor tyrosine kinase
Cerox1	Cytoplasmic endogenous regulator of oxidative phosphorylation 1
Abhd4	Abhydrolase domain-containing 4: *N*-acyl phospholipase B
Plekhm2	Pleckstrin homology and RUN domain containing M2
Sbno2	Strawberry notch homolog 2
Rfxank	Regulatory factor X associated ankyrin containing protein
Dtymk	Deoxythymidylate kinase
Lrrc45	Leucine rich repeat containing 45
Snrnp70	Small nuclear ribonucleoprotein U1 subunit 70
Nrf2	Nuclear factor erythroid-2-related factor 2
GABA	γ-Aminobutyric acid
BBB	Blood brain barrier
ALS	Amyotrophic lateral sclerosis

Author contributions

Conceptualization and data curation: Oh Yoen Kim and Juhyun Song; formal analysis, investigation, and methodology: Danbi Jo, Archana Arjunan, Seoyoon Choi, Yoon Seok Jung, Jihyun Park, Oh Yoen Kim, and Juhyun Song; validation and visualization: Danbi Jo, Oh Yoen Kim, and Juhyun Song; writing – original draft: Danbi Jo, Oh Yoen Kim and Juhyun Song; writing – review and editing: Juhyun Song; funding acquisition and supervision: Oh Yoen Kim and Juhyun Song. All authors have read and approved the final manuscript.

Conflicts of interest

The authors declare no conflicts of interest.

Acknowledgements

This study was supported by the National Research Foundation of Korea (NRF grant 2022R1A2C1006125 to Juhyun Song and 2022R1A2C1010398 to Oh Yoen Kim).

References

1 D. J. Selkoe, Alzheimer's disease: genes, proteins, and therapy, *Physiol. Rev.*, 2001, **81**, 741–766.
2 Y. E. Geda, L. S. Schneider, L. N. Gitlin, D. S. Miller, G. S. Smith, J. Bell, J. Evans, M. Lee, A. Porsteinsson, K. L. Lanctot, P. B. Rosenberg, D. L. Sultzer, P. T. Francis, H. Brodaty, P. P. Padala, C. U. Onyike, L. A. Ortiz, S. Ancoli-Israel, D. L. Bliwise, J. L. Martin, M. V. Vitiello, K. Yaffe, P. C. Zee, N. Herrmann, R. A. Sweet, C. Ballard, N. A. Khin, C. Alfaro, P. S. Murray, S. Schultz, C. G. Lyketsos and I. Neuropsychiatric, Syndromes Professional Interest Area of, Neuropsychiatric symptoms in Alzheimer's disease: past progress and anticipation of the future, *Alzheimers Dement.*, 2013, **9**, 602–608.
3 L. Ferretti, S. M. McCurry, R. Logsdon, L. Gibbons and L. Teri, Anxiety and Alzheimer's disease, *J. Geriatr. Psychiatry Neurol.*, 2001, **14**, 52–58.
4 C. G. Lyketsos, O. Lopez, B. Jones, A. L. Fitzpatrick, J. Breitner and S. DeKosky, Prevalence of neuropsychiatric symptoms in dementia and mild cognitive impairment: results from the cardiovascular health study, *J. Am. Med. Assoc.*, 2002, **288**, 1475–1483.
5 S. Babri, G. Mohaddes, I. Feizi, A. Mohammadnia, A. Niapour, A. Alihemmati and M. Amani, Effect of troxerutin on synaptic plasticity of hippocampal dentate gyrus neurons in a beta-amyloid model of Alzheimer's disease: an electrophysiological study, *Eur. J. Pharmacol.*, 2014, **732**, 19–25.
6 C. Ballard and A. Corbett, Management of neuropsychiatric symptoms in people with dementia, *CNS Drugs*, 2010, **24**, 729–739.
7 A. J. Petkus, C. A. Reynolds, J. L. Wetherell, W. S. Kremen, N. L. Pedersen and M. Gatz, Anxiety is associated with increased risk of dementia in older Swedish twins, *Alzheimers Dement.*, 2016, **12**, 399–406.
8 D. Gallagher, R. Coen, D. Kilroy, K. Belinski, I. Bruce, D. Coakley, B. Walsh, C. Cunningham and B. A. Lawlor, Anxiety and behavioural disturbance as markers of prodromal Alzheimer's disease in patients with mild cognitive impairment, *Int. J. Geriatr. Psychiatry*, 2011, **26**, 166–172.
9 J. N. Perusini and M. S. Fanselow, Neurobehavioral perspectives on the distinction between fear and anxiety, *Learn. Mem.*, 2015, **22**, 417–425.
10 J. P. Aggleton, A. Pralus, A. J. Nelson and M. Hornberger, Thalamic pathology and memory loss in early Alzheimer's disease: moving the focus from the medial temporal lobe to Papez circuit, *Brain*, 2016, **139**, 1877–1890.
11 D. R. Thal, U. Rub, M. Orantes and H. Braak, Phases of A beta-deposition in the human brain and its relevance for the development of AD, *Neurology*, 2002, **58**, 1791–1800.
12 G. W. Van Hoesen, J. C. Augustinack, J. Dierking, S. J. Redman and R. Thangavel, The parahippocampal gyrus in Alzheimer's disease. Clinical and preclinical neuroanatomical correlates, *Ann. N. Y. Acad. Sci.*, 2000, **911**, 254–274.
13 G. A. Carlesimo, F. Piras, M. D. Orfei, M. Iorio, C. Caltagirone and G. Spalletta, Atrophy of presubiculum and subiculum is the earliest hippocampal anatomical marker of Alzheimer's disease, *Alzheimers Dement.*, 2015, **1**, 24–32.
14 J. Zhang, Y. F. Zhen, P. B. C. Ren, L. G. Song, W. N. Kong, T. M. Shao, X. Li and X. Q. Chai, Salidroside attenuates beta amyloid-induced cognitive deficits via modulating oxidative stress and inflammatory mediators in rat hippocampus, *Behav. Brain Res.*, 2013, **244**, 70–81.
15 A. Gella and N. Durany, Oxidative stress in Alzheimer disease, *Cell Adhes. Migr.*, 2009, **3**, 88–93.
16 A. Basli, S. Soulet, N. Chaher, J. M. Merillon, M. Chibane, J. P. Monti and T. Richard, Wine polyphenols: potential agents in neuroprotection, *Oxid. Med. Cell. Longevity*, 2012, **2012**, 805762.
17 A. Dal-Pan, S. Dudonne, P. Bourassa, M. Bourdoulous, C. Tremblay, Y. Desjardins, F. Calon and C. Neurophenols, Cognitive-Enhancing Effects of a Polyphenols-Rich Extract from Fruits without Changes in Neuropathology in an Animal Model of Alzheimer's Disease, *J. Alzheimer's Dis.*, 2017, **55**, 115–135.
18 H. M. Hassan, M. R. Elnagar, E. Abdelrazik, M. R. Mahdi, E. Hamza, E. M. Elattar, E. M. ElNashar, M. A. Alghamdi, Z. Al-Qahtani, K. M. Al-Khater, R. A. Aldahhan and E. L. M, Neuroprotective effect of naringin against cerebellar changes in Alzheimer's disease through modulation of autophagy, oxidative stress and tau expression: An experimental study, *Front. Neuroanat.*, 2022, **16**, 1012422.
19 C. L. Ho, N. J. Kao, C. I. Lin, T. L. Cross and S. H. Lin, Quercetin Increases Mitochondrial Biogenesis and Reduces Free Radicals in Neuronal SH-SY5Y Cells, *Nutrients*, 2022, **14**, 3310.
20 A. A. Gomaa, H. S. M. Farghaly, R. M. Makboul, A. M. Hussien and M. A. Nicola, Polyphenols from Conyza dioscoridis (L.) ameliorate Alzheimer's disease- like alterations through multi-targeting activities in two animal models, *BMC Complementary Med. Ther.*, 2022, **22**, 288.
21 Y. D. Wei, X. X. Chen, L. J. Yang, X. R. Gao, Q. R. Xia, C. C. Qi and J. F. Ge, Resveratrol ameliorates learning and memory impairments induced by bilateral hippocampal injection of streptozotocin in mice, *Neurochem. Int.*, 2022, **159**, 105385.
22 Y. Y. Choi, T. Maeda, H. Fujii, T. Yokozawa, H. Y. Kim, E. J. Cho and T. Shibamoto, Oligonol improves memory and cognition under an amyloid beta(25-35)-induced Alzheimer's mouse model, *Nutr. Res.*, 2014, **34**, 595–603.

23 T. Sakurai, K. Kitadate, H. Nishioka, H. Fujii, J. Ogasawara, T. Kizaki, S. Sato, T. Fujiwara, K. Akagawa, T. Izawa and H. Ohno, Oligomerised lychee fruit-derived polyphenol attenuates cognitive impairment in senescence-accelerated mice and endoplasmic reticulum stress in neuronal cells, *Br. J. Nutr.*, 2013, **110**, 1549–1558.

24 J. S. Noh, C. H. Park and T. Yokozawa, Treatment with oligonol, a low-molecular polyphenol derived from lychee fruit, attenuates diabetes-induced hepatic damage through regulation of oxidative stress and lipid metabolism, *Br. J. Nutr.*, 2011, **106**, 1013–1022.

25 R. Yamanishi, E. Yoshigai, T. Okuyama, M. Mori, H. Murase, T. Machida, T. Okumura and M. Nishizawa, The anti-inflammatory effects of flavanol-rich lychee fruit extract in rat hepatocytes, *PLoS One*, 2014, **9**, e93818.

26 M. Zhang, L. Zhong, X. Han, G. Xiong, D. Xu, S. Zhang, H. Cheng, K. Chiu and Y. Xu, Brain and Retinal Abnormalities in the 5xFAD Mouse Model of Alzheimer's Disease at Early Stages, *Front. Neurosci.*, 2021, **15**, 681831.

27 K. E. Bernstein, Y. Koronyo, B. C. Salumbides, J. Sheyn, L. Pelissier, D. H. Lopes, K. H. Shah, E. A. Bernstein, D. T. Fuchs, J. J. Yu, M. Pham, K. L. Black, X. Z. Shen, S. Fuchs and M. Koronyo-Hamaoui, Angiotensin-converting enzyme overexpression in myelomonocytes prevents Alzheimer's-like cognitive decline, *J. Clin. Invest.*, 2014, **124**, 1000–1012.

28 R. M. Deacon, Digging and marble burying in mice: simple methods for in vivo identification of biological impacts, *Nat. Protoc.*, 2006, **1**, 122–124.

29 S. L. Thompson, A. C. Welch, E. V. Ho, J. M. Bessa, C. Portugal-Nunes, M. Morais, J. W. Young, J. A. Knowles and S. C. Dulawa, Btbd3 expression regulates compulsive-like and exploratory behaviors in mice, *Transl. Psychiatry*, 2019, **9**, 222.

30 N. L. Bray, H. Pimentel, P. Melsted and L. Pachter, Near-optimal probabilistic RNA-seq quantification, *Nat. Biotechnol.*, 2016, **34**, 525–527.

31 M. D. Robinson, D. J. McCarthy and G. K. Smyth, edgeR: a Bioconductor package for differential expression analysis of digital gene expression data, *Bioinformatics*, 2010, **26**, 139–140.

32 A. Liberzon, A. Subramanian, R. Pinchback, H. Thorvaldsdottir, P. Tamayo and J. P. Mesirov, Molecular signatures database (MSigDB) 3.0, *Bioinformatics*, 2011, **27**, 1739–1740.

33 D. Szklarczyk, A. L. Gable, D. Lyon, A. Junge, S. Wyder, J. Huerta-Cepas, M. Simonovic, N. T. Doncheva, J. H. Morris, P. Bork, L. J. Jensen and C. V. Mering, STRING v11: protein-protein association networks with increased coverage, supporting functional discovery in genome-wide experimental datasets, *Nucleic Acids Res.*, 2019, **47**, D607–D613.

34 S. Oddo, A. Caccamo, J. D. Shepherd, M. P. Murphy, T. E. Golde, R. Kayed, R. Metherate, M. P. Mattson, Y. Akbari and F. M. LaFerla, Triple-transgenic model of Alzheimer's disease with plaques and tangles: intracellular Abeta and synaptic dysfunction, *Neuron*, 2003, **39**, 409–421.

35 H. Oakley, S. L. Cole, S. Logan, E. Maus, P. Shao, J. Craft, A. Guillozet-Bongaarts, M. Ohno, J. Disterhoft, L. Van Eldik, R. Berry and R. Vassar, Intraneuronal beta-amyloid aggregates, neurodegeneration, and neuron loss in transgenic mice with five familial Alzheimer's disease mutations: potential factors in amyloid plaque formation, *J. Neurosci.*, 2006, **26**, 10129–10140.

36 H. K. Bhakta, P. Paudel, H. Fujii, A. Sato, C. H. Park, T. Yokozawa, H. A. Jung and J. S. Choi, Oligonol promotes glucose uptake by modulating the insulin signaling pathway in insulin-resistant HepG2 cells via inhibiting protein tyrosine phosphatase 1B, *Arch. Pharmacal Res.*, 2017, **40**, 1314–1327.

37 M. Mani, S. Khaghani, T. Gol Mohammadi, Z. Zamani, K. Azadmanesh, R. Meshkani, P. Pasalar and E. Mostafavi, Activation of Nrf2-Antioxidant Response Element Mediated Glutamate Cysteine Ligase Expression in Hepatoma Cell line by Homocysteine, *Hepatitis Mon.*, 2013, **13**, e8394.

38 E. N. Terry, P. H. Gann, R. Molokie, M. Deininger and A. M. Diamond, Changes in the activity of the GPx-1 antioxidant selenoenzyme in mononuclear cells following imatinib treatment, *Leuk. Res.*, 2011, **35**, 831–833.

39 V. Srivastava, B. Buzas, R. Momenan, G. Oroszi, A. J. Pulay, M. A. Enoch, D. W. Hommer and D. Goldman, Association of SOD2, a mitochondrial antioxidant enzyme, with gray matter volume shrinkage in alcoholics, *Neuropsychopharmacology*, 2010, **35**, 1120–1128.

40 Y. Zhang, Y. Xu, W. Lu, J. Li, S. Yu, E. J. Brown, B. Z. Stanger, J. D. Rabinowitz and X. Yang, G6PD-mediated increase in de novo NADP(+) biosynthesis promotes antioxidant defense and tumor metastasis, *Sci. Adv.*, 2022, **8**, eabo0404.

41 Z. Zhang, J. Qu, C. Zheng, P. Zhang, W. Zhou, W. Cui, X. Mo, L. Li, L. Xu and J. Gao, Nrf2 antioxidant pathway suppresses Numb-mediated epithelial-mesenchymal transition during pulmonary fibrosis, *Cell Death Dis.*, 2018, **9**, 83.

42 J. A. Godoy-Lugo, M. A. Thorwald, D. A. Mendez, R. Rodriguez, D. Nakano, A. Nishiyama and R. M. Ortiz, Glucose Increases Hepatic Mitochondrial Antioxidant Enzyme Activities in Insulin Resistant Rats Following Chronic Angiotensin Receptor Blockade, *Int. J. Mol. Sci.*, 2022, **23**, 10897.

43 Y. C. Kuo, I. Y. Chen, S. C. Chang, S. C. Wu, T. M. Hung, P. H. Lee, K. Shimotohno and M. F. Chang, Hepatitis C virus NS5A protein enhances gluconeogenesis through upregulation of Akt-/JNK-PEPCK signalling pathways, *Liver Int.*, 2014, **34**, 1358–1368.

44 B. Onken, N. Kalinava and M. Driscoll, Gluconeogenesis and PEPCK are critical components of healthy aging and dietary restriction life extension, *PLoS Genet.*, 2020, **16**, e1008982.

45 I. Valle, A. Alvarez-Barrientos, E. Arza, S. Lamas and M. Monsalve, PGC-1alpha regulates the mitochondrial antioxidant defense system in vascular endothelial cells, *Cardiovasc. Res.*, 2005, **66**, 562–573.
46 A. M. Tormos, S. Perez-Garrido, R. Talens-Visconti, A. R. Nebreda and J. Sastre, Long term p38-a deficiency up-regulates antioxidant enzymes through compensatory NF-?B activation, *Free Radicals Biol. Med.*, 2014, **75**(Suppl 1), S52.
47 J. Iacovelli, G. C. Rowe, A. Khadka, D. Diaz-Aguilar, C. Spencer, Z. Arany and M. Saint-Geniez, PGC-1alpha Induces Human RPE Oxidative Metabolism and Antioxidant Capacity, *Invest. Ophthalmol. Visual Sci.*, 2016, **57**, 1038–1051.
48 Y. Suzuki and I. Imayoshi, Network analysis of exploratory behaviors of mice in a spatial learning and memory task, *PLoS One*, 2017, **12**, e0180789.
49 T. Illouz, R. Madar and E. Okun, A modified Barnes maze for an accurate assessment of spatial learning in mice, *J. Neurosci. Methods*, 2020, **334**, 108579.
50 C. A. Barnes, Memory deficits associated with senescence: a neurophysiological and behavioral study in the rat, *J. Comp. Physiol. Psychol.*, 1979, **93**, 74–104.
51 F. P. Varodayan, H. Sidhu, M. Kreifeldt, M. Roberto and C. Contet, Morphological and functional evidence of increased excitatory signaling in the prelimbic cortex during ethanol withdrawal, *Neuropharmacology*, 2018, **133**, 470–480.
52 K. Gawel, E. Gibula, M. Marszalek-Grabska, J. Filarowska and J. H. Kotlinska, Assessment of spatial learning and memory in the Barnes maze task in rodents-methodological consideration, *Naunyn Schmiedebergs Arch. Pharmacol.*, 2019, **392**, 1–18.
53 A. Attar, T. Liu, W. T. Chan, J. Hayes, M. Nejad, K. Lei and G. Bitan, A shortened Barnes maze protocol reveals memory deficits at 4-months of age in the triple-transgenic mouse model of Alzheimer's disease, *PLoS One*, 2013, **8**, e80355.
54 T. P. O'Leary and R. E. Brown, Visuo-spatial learning and memory deficits on the Barnes maze in the 16-month-old APPswe/PS1dE9 mouse model of Alzheimer's disease, *Behav. Brain Res.*, 2009, **201**, 120–127.
55 K. Njung'e and S. L. Handley, Evaluation of marble-burying behavior as a model of anxiety, *Pharmacol., Biochem. Behav.*, 1991, **38**, 63–67.
56 G. T. Taylor, S. Lerch and S. Chourbaji, Marble burying as compulsive behaviors in male and female mice, *Acta Neurobiol. Exp.*, 2017, **77**, 254–260.
57 C. L. Broekkamp, H. W. Rijk, D. Joly-Gelouin and K. L. Lloyd, Major tranquillizers can be distinguished from minor tranquillizers on the basis of effects on marble burying and swim-induced grooming in mice, *Eur. J. Pharmacol.*, 1986, **126**, 223–229.
58 V. Torres-Lista, S. Lopez-Pousa and L. Gimenez-Llort, Marble-burying is enhanced in 3xTg-AD mice, can be reversed by risperidone and it is modulable by handling, *Behav. Processes*, 2015, **116**, 69–74.
59 V. Torres-Lista and L. Gimenez-Llort, Impairment of nesting behaviour in 3xTg-AD mice, *Behav. Brain Res.*, 2013, **247**, 153–157.
60 F. Dorninger, G. Zeitler and J. Berger, Nestlet Shredding and Nest Building Tests to Assess Features of Psychiatric Disorders in Mice, *Bio-Protoc.*, 2020, **10**, e3863.
61 P. Jirkof, Burrowing and nest building behavior as indicators of well-being in mice, *J. Neurosci. Methods*, 2014, **234**, 139–146.
62 M. Angoa-Perez, M. J. Kane, D. I. Briggs, D. M. Francescutti and D. M. Kuhn, Marble burying and nestlet shredding as tests of repetitive, compulsive-like behaviors in mice, *J. Visualized Exp.*, 2013, 50978, DOI: 10.3791/50978.
63 T. N. Sager, J. Kirchhoff, A. Mork, J. Van Beek, K. Thirstrup, M. Didriksen and J. B. Lauridsen, Nest building performance following MPTP toxicity in mice, *Behav. Brain Res.*, 2010, **208**, 444–449.
64 R. M. Deacon, A. Croucher and J. N. Rawlins, Hippocampal cytotoxic lesion effects on species-typical behaviours in mice, *Behav. Brain Res.*, 2002, **132**, 203–213.
65 J. Hannon and D. Hoyer, Molecular biology of 5-HT receptors, *Behav. Brain Res.*, 2008, **195**, 198–213.
66 C. Bombardi, Neuronal localization of the 5-HT2 receptor family in the amygdaloid complex, *Front. Pharmacol.*, 2014, **5**, 68.
67 J. Versijpt, K. J. Van Laere, F. Dumont, D. Decoo, M. Vandecapelle, P. Santens, I. Goethals, K. Audenaert, G. Slegers, R. A. Dierckx and J. Korf, Imaging of the 5-HT2A system: age-, gender-, and Alzheimer's disease-related findings, *Neurobiol. Aging*, 2003, **24**, 553–561.
68 S. Khaliq, S. Haider, S. P. Ahmed, T. Perveen and D. J. Haleem, Relationship of brain tryptophan and serotonin in improving cognitive performance in rats, *Pak. J. Pharm. Sci.*, 2006, **19**, 11–15.
69 L. Marner, V. G. Frokjaer, J. Kalbitzer, S. Lehel, K. Madsen, W. F. Baare, G. M. Knudsen and S. G. Hasselbalch, Loss of serotonin 2A receptors exceeds loss of serotonergic projections in early Alzheimer's disease: a combined [11C]DASB and [18F]altanserin-PET study, *Neurobiol. Aging*, 2012, **33**, 479–487.
70 D. Sierra-Mercado, N. Padilla-Coreano and G. J. Quirk, Dissociable roles of prelimbic and infralimbic cortices, ventral hippocampus, and basolateral amygdala in the expression and extinction of conditioned fear, *Neuropsychopharmacology*, 2011, **36**, 529–538.
71 G. Zhang, H. N. Asgeirsdottir, S. J. Cohen, A. H. Munchow, M. P. Barrera and R. W. Stackman Jr., Stimulation of serotonin 2A receptors facilitates consolidation and extinction of fear memory in C57BL/6J mice, *Neuropharmacology*, 2013, **64**, 403–413.
72 G. J. Quirk, D. Pare, R. Richardson, C. Herry, M. H. Monfils, D. Schiller and A. Vicentic, Erasing fear memories with extinction training, *J. Neurosci.*, 2010, **30**, 14993–14997.

73 C. S. Grob, A. L. Danforth, G. S. Chopra, M. Hagerty, C. R. McKay, A. L. Halberstadt and G. R. Greer, Pilot study of psilocybin treatment for anxiety in patients with advanced-stage cancer, *Arch. Gen. Psychiatry*, 2011, **68**, 71–78.

74 K. A. Jones, D. P. Srivastava, J. A. Allen, R. T. Strachan, B. L. Roth and P. Penzes, Rapid modulation of spine morphology by the 5-HT2A serotonin receptor through kalirin-7 signaling, *Proc. Natl. Acad. Sci. U. S. A.*, 2009, **106**, 19575–19580.

75 Z. Xia, J. A. Gray, B. A. Compton-Toth and B. L. Roth, A direct interaction of PSD-95 with 5-HT2A serotonin receptors regulates receptor trafficking and signal transduction, *J. Biol. Chem.*, 2003, **278**, 21901–21908.

76 M. J. Millan, P. Marin, J. Bockaert and C. Mannoury la Cour, Signaling at G-protein-coupled serotonin receptors: recent advances and future research directions, *Trends Pharmacol. Sci.*, 2008, **29**, 454–464.

77 Y. Yan, J. Wang, B. Qu, Y. Zhang, Y. Wei, H. Liu and C. Wu, CXCL13 and TH1/Th2 cytokines in the serum and cerebrospinal fluid of neurosyphilis patients, *Medicine*, 2017, **96**, e8850.

78 K. E. Cole, C. A. Strick, T. J. Paradis, K. T. Ogborne, M. Loetscher, R. P. Gladue, W. Lin, J. G. Boyd, B. Moser, D. E. Wood, B. G. Sahagan and K. Neote, Interferon-inducible T cell alpha chemoattractant (I-TAC): a novel non-ELR CXC chemokine with potent activity on activated T cells through selective high affinity binding to CXCR3, *J. Exp. Med.*, 1998, **187**, 2009–2021.

79 Z. Beizavi, M. Zohouri, M. Asadipour and A. Ghaderi, IL-27, a pleiotropic cytokine for fine-tuning the immune response in cancer, *Int. Rev. Immunol.*, 2021, **40**, 319–329.

80 L. B. Ivashkiv, IFNgamma: signalling, epigenetics and roles in immunity, metabolism, disease and cancer immunotherapy, *Nat. Rev. Immunol.*, 2018, **18**, 545–558.

81 N. R. West, A. N. Hegazy, B. M. J. Owens, S. J. Bullers, B. Linggi, S. Buonocore, M. Coccia, D. Gortz, S. This, K. Stockenhuber, J. Pott, M. Friedrich, G. Ryzhakov, F. Baribaud, C. Brodmerkel, C. Cieluch, N. Rahman, G. Muller-Newen, R. J. Owens, A. A. Kuhl, K. J. Maloy, S. E. Plevy, Oxford IBD Cohort Investigators, S. Keshav, S. P. L. Travis and F. Powrie, Oncostatin M drives intestinal inflammation and predicts response to tumor necrosis factor-neutralizing therapy in patients with inflammatory bowel disease, *Nat. Med.*, 2017, **23**, 579–589.

82 F. Vafaee, A. Zarifkar, M. Emamghoreishi, M. R. Namavar, S. Shirzad, H. Ghazavi and V. Mahdavizadeh, Insulin-Like Growth Factor 2 (IGF-2) Regulates Neuronal Density and IGF-2 Distribution Following Hippocampal Intracerebral Hemorrhage, *J. Stroke Cerebrovasc. Dis.*, 2020, **29**, 105128.

83 H. Jia, J. Cheng, Q. Zhou, J. Peng, Y. Pan and H. Han, Fibroblast growth factor 21 attenuates inflammation and oxidative stress in atherosclerotic rat via enhancing the Nrf1-ARE signaling pathway, *Int. J. Clin. Exp. Pathol.*, 2018, **11**, 1308–1317.

84 M. H. Qiu, M. C. Chen, Z. L. Huang and J. Lu, Neuronal activity (c-Fos) delineating interactions of the cerebral cortex and basal ganglia, *Front. Neuroanat.*, 2014, **8**, 13.

85 E. Knapska and S. Maren, Reciprocal patterns of c-Fos expression in the medial prefrontal cortex and amygdala after extinction and renewal of conditioned fear, *Learn. Mem.*, 2009, **16**, 486–493.

86 Y. Sun, H. Zhu, R. Cheng, Z. Tang and M. Zhang, Outer membrane protein Amuc_1100 of Akkermansia muciniphila alleviates antibiotic-induced anxiety and depression-like behavior in mice, *Physiol. Behav.*, 2023, **258**, 114023.

87 C. L. Ge, W. Chen, L. N. Zhang, Y. H. Ai, Y. Zou and Q. Y. Peng, Hippocampus-prefrontal cortex inputs modulate spatial learning and memory in a mouse model of sepsis induced by cecal ligation puncture, *CNS Neurosci. Ther.*, 2023, **29**, 390–401.

88 K. S. Yoo, K. Lee, J. Y. Oh, H. Lee, H. Park, Y. S. Park and H. K. Kim, Postsynaptic density protein 95 (PSD-95) is transported by KIF5 to dendritic regions, *Mol. Brain*, 2019, **12**, 97.

89 M. J. Broadhead, M. H. Horrocks, F. Zhu, L. Muresan, R. Benavides-Piccione, J. DeFelipe, D. Fricker, M. V. Kopanitsa, R. R. Duncan, D. Klenerman, N. H. Komiyama, S. F. Lee and S. G. Grant, PSD95 nanoclusters are postsynaptic building blocks in hippocampus circuits, *Sci. Rep.*, 2016, **6**, 24626.

90 K. S. Christopherson, N. T. Sweeney, S. E. Craven, R. Kang, D. El-Husseini Ael and D. S. Bredt, Lipid- and protein-mediated multimerization of PSD-95: implications for receptor clustering and assembly of synaptic protein networks, *J. Cell Sci.*, 2003, **116**, 3213–3219.

91 A. Yoshii and M. Constantine-Paton, Postsynaptic localization of PSD-95 is regulated by all three pathways downstream of TrkB signaling, *Front. Synaptic Neurosci.*, 2014, **6**, 6.

92 Y. Li, H. Wang, Y. Gao, R. Zhang, Q. Liu, W. Xie, Z. Liu, D. Geng and L. Wang, Circ-Vps41 positively modulates Syp and its overexpression improves memory ability in aging mice, *Front. Mol. Neurosci.*, 2022, **15**, 1037912.

93 A. K. Jyothi, B. Thotakura, S. C. Priyadarshini, S. Patil, M. S. Poojari and M. Subramanian, Paternal stress alters synaptic density and expression of GAP-43, GRIN1, M1 and SYP genes in the hippocampus and cortex of offspring of stress-induced male rats, *Morphologie*, 2022, **107**, 67–79.

94 A. Karimani, N. Ramezani, A. Afkhami Goli, M. H. Nazem Shirazi, H. Nourani and A. M. Jafari, Subchronic neurotoxicity of diazinon in albino mice: Impact of oxidative stress, AChE activity, and gene expression disturbances in the cerebral cortex and hippocampus on mood, spatial learning, and memory function, *Toxicol. Rep.*, 2021, **8**, 1280–1288.

95 X. M. Qi, L. L. Miao, Y. Cai, L. K. Gong and J. Ren, ROS generated by CYP450, especially CYP2E1, mediate mito-

chondrial dysfunction induced by tetrandrine in rat hepatocytes, *Acta Pharmacol. Sin.*, 2013, **34**, 1229–1236.

96 A. Veith and B. Moorthy, Role of Cytochrome P450s in the Generation and Metabolism of Reactive Oxygen Species, *Curr. Opin. Toxicol.*, 2018, **7**, 44–51.

97 L. T. Knapp and E. Klann, Role of reactive oxygen species in hippocampal long-term potentiation: contributory or inhibitory?, *J. Neurosci. Res.*, 2002, **70**, 1–7.

98 P. Liu, J. Wang, S. Peng, D. Zhang, L. Zhuang, C. Liu, Y. Zhang and X. Shi, Suppression of phosphodiesterase IV enzyme by roflumilast ameliorates cognitive dysfunction in aged rats after sevoflurane anaesthesia via PKA-CREB and MEK/ERK pathways, *Eur. J. Neurosci.*, 2022, **56**, 4317–4332.

99 X. X. Xu, R. X. Shi, Y. Fu, J. L. Wang, X. Tong, S. Q. Zhang, N. Wang, M. X. Li, Y. Tong, W. Wang, M. He, B. Y. Liu, G. L. Chen and F. Guo, Neuronal nitric oxide synthase/reactive oxygen species pathway is involved in apoptosis and pyroptosis in epilepsy, *Neural Regener. Res.*, 2023, **18**, 1277–1285.

100 L. F. Liu, Y. Hu, Y. N. Liu, D. W. Shi, C. Liu, X. Da, S. H. Zhu, Q. Y. Zhu, J. Q. Zhang and G. H. Xu, Reactive oxygen species contribute to delirium-like behavior by activating CypA/MMP9 signaling and inducing blood-brain barrier impairment in aged mice following anesthesia and surgery, *Front. Aging Neurosci.*, 2022, **14**, 1021129.

101 S. S. Schattauer, A. Bedini, F. Summers, A. Reilly-Treat, M. M. Andrews, B. B. Land and C. Chavkin, Reactive oxygen species (ROS) generation is stimulated by kappa opioid receptor activation through phosphorylated c-Jun N-terminal kinase and inhibited by p38 mitogen-activated protein kinase (MAPK) activation, *J. Biol. Chem.*, 2019, **294**, 16884–16896.

102 K. J. Cho, H. W. Kim, S. Y. Cheon, J. E. Lee and G. W. Kim, Apoptosis signal-regulating kinase-1 aggravates ROS-mediated striatal degeneration in 3-nitropropionic acid-infused mice, *Biochem. Biophys. Res. Commun.*, 2013, **441**, 280–285.

103 L. Amador-Alvarado, T. Montiel and L. Massieu, Differential production of reactive oxygen species in distinct brain regions of hypoglycemic mice, *Metab. Brain Dis.*, 2014, **29**, 711–719.

104 T. Kitada, A. Pisani, D. R. Porter, H. Yamaguchi, A. Tscherter, G. Martella, P. Bonsi, C. Zhang, E. N. Pothos and J. Shen, Impaired dopamine release and synaptic plasticity in the striatum of PINK1-deficient mice, *Proc. Natl. Acad. Sci. U. S. A.*, 2007, **104**, 11441–11446.

105 A. S. Gravesteijn, H. Beckerman, E. A. Willemse, H. E. Hulst, B. A. de Jong, C. E. Teunissen and V. de Groot, Brain-derived neurotrophic factor, neurofilament light and glial fibrillary acidic protein do not change in response to aerobic training in people with MS-related fatigue - a secondary analysis of a randomized controlled trial, *Mult. Scler. Relat. Disord.*, 2022, **70**, 104489.

106 A. D. Garcia, N. B. Doan, T. Imura, T. G. Bush and M. V. Sofroniew, GFAP-expressing progenitors are the principal source of constitutive neurogenesis in adult mouse forebrain, *Nat. Neurosci.*, 2004, **7**, 1233–1241.

107 C. Li, Y. Zhu, Y. Wu, M. Fu, Y. Wu, Y. Wu, Y. Qiu, H. Zhang and M. Ding, Oridonin Alleviates LPS-Induced Depression by Inhibiting NLRP3 Inflammasome via Activation of Autophagy, *Front. Med.*, 2021, **8**, 813047.

108 Y. Ying, G. Xiang, M. Chen, J. Ye, Q. Wu, H. Dou, S. Sheng and S. Zhu, Gelatine nanostructured lipid carrier encapsulated FGF15 inhibits autophagy and improves recovery in spinal cord injury, *Cell Death Discovery*, 2020, **6**, 137.

109 C. Habak, A. Noreau, A. Nagano-Saito, B. Mejia-Constain, C. Degroot, A. P. Strafella, S. Chouinard, A. L. Lafontaine, G. A. Rouleau and O. Monchi, Dopamine transporter SLC6A3 genotype affects cortico-striatal activity of set-shifts in Parkinson's disease, *Brain*, 2014, **137**, 3025–3035.

110 M. E. A. Reith, S. Kortagere, C. E. Wiers, H. Sun, M. A. Kurian, A. Galli, N. D. Volkow and Z. Lin, The dopamine transporter gene SLC6A3: multidisease risks, *Mol. Psychiatry*, 2022, **27**, 1031–1046.

111 D. J. Walther, J. U. Peter, S. Bashammakh, H. Hortnagl, M. Voits, H. Fink and M. Bader, Synthesis of serotonin by a second tryptophan hydroxylase isoform, *Science*, 2003, **299**, 76.

112 L. Gutknecht, N. Araragi, S. Merker, J. Waider, F. M. Sommerlandt, B. Mlinar, G. Baccini, U. Mayer, F. Proft, M. Hamon, A. G. Schmitt, R. Corradetti, L. Lanfumey and K. P. Lesch, Impacts of brain serotonin deficiency following Tph2 inactivation on development and raphe neuron serotonergic specification, *PLoS One*, 2012, **7**, e43157.

113 F. Wasinski, M. R. Tavares, D. O. Gusmao, E. O. List, J. J. Kopchick, G. A. Alves, R. Frazao and J. Donato Jr., Central growth hormone action regulates neuroglial and proinflammatory markers in the hypothalamus of male mice, *Neurosci. Lett.*, 2023, **806**, 137236.

114 B. Guo, M. Qi, S. Huang, R. Zhuo, W. Zhang, Y. Zhang, M. Xu, M. Liu, T. Guan and Y. Liu, Cadherin-12 Regulates Neurite Outgrowth Through the PKA/Rac1/Cdc42 Pathway in Cortical Neurons, *Front. Cell Dev. Biol.*, 2021, **9**, 768970.

115 J. B. Regard, S. Scheek, T. Borbiev, A. A. Lanahan, A. Schneider, A. M. Demetriades, H. Hiemisch, C. A. Barnes, A. D. Verin and P. F. Worley, Verge: a novel vascular early response gene, *J. Neurosci.*, 2004, **24**, 4092–4103.

116 Z. Fan, R. Ardicoglu, A. A. Batavia, R. Rust, L. von Ziegler, R. Waag, J. Zhang, T. Desgeorges, O. Sturman, H. Dang, R. Weber, M. Roszkowski, A. E. Moor, M. E. Schwab, P. L. Germain, J. Bohacek and K. De Bock, The vascular gene Apold1 is dispensable for normal development but controls angiogenesis under pathological conditions, *Angiogenesis*, 2023, **26**, 385–407.

117 J. H. Chen, M. Segni, F. Payne, I. Huang-Doran, A. Sleigh, C. Adams, U. K. Consortium, D. B. Savage, S. O'Rahilly, R. K. Semple and I. Barroso, Truncation of POC1A associated with short stature and extreme insulin resistance, *J. Mol. Endocrinol.*, 2015, **55**, 147–158.

118 X. Wang, Y. Su, H. Yan, Z. Huang, Y. Huang and W. Yue, Association Study of KCNH7 Polymorphisms and Individual Responses to Risperidone Treatment in Schizophrenia, *Front. Psychiatry*, 2019, **10**, 633.

119 J. Gao, Z. Qin, X. Qu, S. Wu, X. Xie, C. Liang and J. Liu, Endogenous neuroprotective mechanism of ATP2B1 in transcriptional regulation of ischemic preconditioning, *Am. J. Transl. Res.*, 2021, **13**, 1170–1183.

120 A. A. Sultan, M. K. Dimick, C. C. Zai, J. L. Kennedy, B. J. MacIntosh and B. I. Goldstein, The association of CNR1 genetic variants with resting-state functional connectivity in youth bipolar disorder, *Eur. Neuropsychopharmacol.*, 2023, **71**, 41–54.

121 C. Leukel, D. Schumann, R. Kalisch, T. Sommer and N. Bunzeck, Dopamine Related Genes Differentially Affect Declarative Long-Term Memory in Healthy Humans, *Front. Behav. Neurosci.*, 2020, **14**, 539725.

122 H. Fukushima, R. Maeda, R. Suzuki, A. Suzuki, M. Nomoto, H. Toyoda, L. J. Wu, H. Xu, M. G. Zhao, K. Ueda, A. Kitamoto, N. Mamiya, T. Yoshida, S. Homma, S. Masushige, M. Zhuo and S. Kida, Upregulation of calcium/calmodulin-dependent protein kinase IV improves memory formation and rescues memory loss with aging, *J. Neurosci.*, 2008, **28**, 9910–9919.

123 L. Galvan, L. Francelle, M. C. Gaillard, L. de Longprez, M. A. Carrillo-de Sauvage, G. Liot, K. Cambon, L. Stimmer, S. Luccantoni, J. Flament, J. Valette, M. de Chaldee, G. Auregan, M. Guillermier, C. Josephine, F. Petit, C. Jan, M. Jarrige, N. Dufour, G. Bonvento, S. Humbert, F. Saudou, P. Hantraye, K. Merienne, A. P. Bemelmans, A. L. Perrier, N. Deglon and E. Brouillet, The striatal kinase DCLK3 produces neuroprotection against mutant huntingtin, *Brain*, 2018, **141**, 1434–1454.

124 R. Bonate, G. Kurek, M. Hrabak, S. Patterson, F. Padovan-Neto, A. R. West and H. Steiner, Phosphodiesterase 10A (PDE10A): Regulator of Dopamine Agonist-Induced Gene Expression in the Striatum, *Cells*, 2022, **11**, 2214.

125 E. Schwarz, A gene-based review of RGS4 as a putative risk gene for psychiatric illness, *Am. J. Med. Genet., Part B*, 2018, **177**, 267–273.

126 M. Stratinaki, A. Varidaki, V. Mitsi, S. Ghose, J. Magida, C. Dias, S. J. Russo, V. Vialou, B. J. Caldarone, C. A. Tamminga, E. J. Nestler and V. Zachariou, Regulator of G protein signaling 4 [corrected] is a crucial modulator of antidepressant drug action in depression and neuropathic pain models, *Proc. Natl. Acad. Sci. U. S. A.*, 2013, **110**, 8254–8259.

127 C. D. Paspalas, L. D. Selemon and A. F. Arnsten, Mapping the regulator of G protein signaling 4 (RGS4): presynaptic and postsynaptic substrates for neuroregulation in prefrontal cortex, *Cereb. Cortex*, 2009, **19**, 2145–2155.

128 P. D. Negraes, C. A. Trujillo, N. K. Yu, W. Wu, H. Yao, N. Liang, J. D. Lautz, E. Kwok, D. McClatchy, J. Diedrich, S. M. de Bartolome, J. Truong, R. Szeto, T. Tran, R. H. Herai, S. E. P. Smith, G. G. Haddad, J. R. Yates 3rd and A. R. Muotri, Altered network and rescue of human neurons derived from individuals with early-onset genetic epilepsy, *Mol. Psychiatry*, 2021, **26**, 7047–7068.

129 J. Zhao, C. Chen, R. L. Bell, H. Qing and Z. Lin, Identification of HIVEP2 as a dopaminergic transcription factor related to substance use disorders in rats and humans, *Transl. Psychiatry*, 2019, **9**, 247.

130 H. Melland, F. Bumbak, A. Kolesnik-Taylor, E. Ng-Cordell, A. John, P. Constantinou, S. Joss, M. Larsen, C. Fagerberg, L. W. Laulund, J. Thies, F. Emslie, M. Willemsen, T. Kleefstra, R. Pfundt, R. Barrick, R. Chang, L. Loong, M. Alfadhel, J. van der Smagt, M. Nizon, M. A. Kurian, D. J. Scott, J. J. Ziarek, S. L. Gordon and K. Baker, Expanding the genotype and phenotype spectrum of SYT1-associated neurodevelopmental disorder, *Genet. Med.*, 2022, **24**, 880–893.

131 S. Awasthi, A. Hindle, N. A. Sawant, M. George, M. Vijayan, S. Kshirsagar, H. Morton, L. E. Bunquin, P. T. Palade, J. J. Lawrence, H. Khan, C. Bose, P. H. Reddy and S. P. Singh, RALBP1 in Oxidative Stress and Mitochondrial Dysfunction in Alzheimer's Disease, *Cells*, 2021, **10**, 3113.

132 B. Bennani-Baiti, S. Toegel, H. Viernstein, E. Urban, C. R. Noe and I. M. Bennani-Baiti, Inflammation Modulates RLIP76/RALBP1 Electrophile-Glutathione Conjugate Transporter and Housekeeping Genes in Human Blood-Brain Barrier Endothelial Cells, *PLoS One*, 2015, **10**, e0139101.

133 R. Tripathi, T. Aggarwal and R. Fredriksson, SLC38A10 Transporter Plays a Role in Cell Survival Under Oxidative Stress and Glutamate Toxicity, *Front. Mol. Biosci.*, 2021, **8**, 671865.

134 E. R. Doroshenko, P. C. Drohomyrecky, A. Gower, H. Whetstone, L. S. Cahill, M. Ganguly, S. Spring, T. J. Yi, J. G. Sled and S. E. Dunn, Peroxisome Proliferator-Activated Receptor-delta Deficiency in Microglia Results in Exacerbated Axonal Injury and Tissue Loss in Experimental Autoimmune Encephalomyelitis, *Front. Immunol.*, 2021, **12**, 570425.

135 L. Wang, X. Wang, Z. Li, T. Xia, L. Zhu, B. Liu, Y. Zhang, F. Xiao, Y. Pan, Y. Liu, F. Guo and Y. Chen, PAQR3 has modulatory roles in obesity, energy metabolism, and leptin signaling, *Endocrinology*, 2013, **154**, 4525–4535.

136 T. Huang, L. Fang, R. He, H. Weng, X. Chen, Q. Ye and D. Qu, Fbxo7 and Pink1 play a reciprocal role in regulating their protein levels, *Aging*, 2020, **13**, 77–88.

137 M. Correa-Vela, V. Lupo, M. Montpeyo, P. Sancho, A. Marce-Grau, J. Hernandez-Vara, A. Darling, A. Jenkins, S. Fernandez-Rodriguez, C. Tello, L. Ramirez-Jimenez, B. Perez, A. Sanchez-Montanez, A. Macaya, M. J. Sobrido, M. Martinez-Vicente, B. Perez-Duenas and C. Espinos, Impaired proteasome activity and neurodegeneration with brain iron accumulation in FBXO7 defect, *Ann. Clin. Transl. Neurol.*, 2020, **7**, 1436–1442.

138 H. Long, X. Zhu, P. Yang, Q. Gao, Y. Chen and L. Ma, Myo9b and RICS modulate dendritic morphology of cortical neurons, *Cereb. Cortex*, 2013, **23**, 71–79.

139 P. Hollingworth, D. Harold, R. Sims, A. Gerrish, J. C. Lambert, M. M. Carrasquillo, R. Abraham,

M. L. Hamshere, J. S. Pahwa, V. Moskvina, K. Dowzell, N. Jones, A. Stretton, C. Thomas, A. Richards, D. Ivanov, C. Widdowson, J. Chapman, S. Lovestone, J. Powell, P. Proitsi, M. K. Lupton, C. Brayne, D. C. Rubinsztein, M. Gill, B. Lawlor, A. Lynch, K. S. Brown, P. A. Passmore, D. Craig, B. McGuinness, S. Todd, C. Holmes, D. Mann, A. D. Smith, H. Beaumont, D. Warden, G. Wilcock, S. Love, P. G. Kehoe, N. M. Hooper, E. R. Vardy, J. Hardy, S. Mead, N. C. Fox, M. Rossor, J. Collinge, W. Maier, F. Jessen, E. Ruther, B. Schurmann, R. Heun, H. Kolsch, H. van den Bussche, I. Heuser, J. Kornhuber, J. Wiltfang, M. Dichgans, L. Frolich, H. Hampel, J. Gallacher, M. Hull, D. Rujescu, I. Giegling, A. M. Goate, J. S. Kauwe, C. Cruchaga, P. Nowotny, J. C. Morris, K. Mayo, K. Sleegers, K. Bettens, S. Engelborghs, P. P. De Deyn, C. Van Broeckhoven, G. Livingston, N. J. Bass, H. Gurling, A. McQuillin, R. Gwilliam, P. Deloukas, A. Al-Chalabi, C. E. Shaw, M. Tsolaki, A. B. Singleton, R. Guerreiro, T. W. Muhleisen, M. M. Nothen, S. Moebus, K. H. Jockel, N. Klopp, H. E. Wichmann, V. S. Pankratz, S. B. Sando, J. O. Aasly, M. Barcikowska, Z. K. Wszolek, D. W. Dickson, N. R. Graff-Radford, R. C. Petersen, Alzheimer's Disease Neuroimaging Initiative, C. M. van Duijn, M. M. Breteler, M. A. Ikram, A. L. DeStefano, A. L. Fitzpatrick, O. Lopez, L. J. Launer, S. Seshadri, C. Consortium, C. Berr, D. Campion, J. Epelbaum, J. F. Dartigues, C. Tzourio, A. Alperovitch, M. Lathrop, E. Consortium, T. M. Feulner, P. Friedrich, C. Riehle, M. Krawczak, S. Schreiber, M. Mayhaus, S. Nicolhaus, S. Wagenpfeil, S. Steinberg, H. Stefansson, K. Stefansson, J. Snaedal, S. Bjornsson, P. V. Jonsson, V. Chouraki, B. Genier-Boley, M. Hiltunen, H. Soininen, O. Combarros, D. Zelenika, M. Delepine, M. J. Bullido, F. Pasquier, I. Mateo, A. Frank-Garcia, E. Porcellini, O. Hanon, E. Coto, V. Alvarez, P. Bosco, G. Siciliano, M. Mancuso, F. Panza, V. Solfrizzi, B. Nacmias, S. Sorbi, P. Bossu, P. Piccardi, B. Arosio, G. Annoni, D. Seripa, A. Pilotto, E. Scarpini, D. Galimberti, A. Brice, D. Hannequin, F. Licastro, L. Jones, P. A. Holmans, T. Jonsson, M. Riemenschneider, K. Morgan, S. G. Younkin, M. J. Owen, M. O'Donovan, P. Amouyel and J. Williams, Common variants at ABCA7, MS4A6A/MS4A4E, EPHA1, CD33 and CD2AP are associated with Alzheimer's disease, *Nat. Genet.*, 2011, **43**, 429–435.

140 S. Dib, J. Pahnke and F. Gosselet, Role of ABCA7 in Human Health and in Alzheimer's Disease, *Int. J. Mol. Sci.*, 2021, **22**, 4603.

141 T. E. Syme, M. Grill, E. Hayashida, B. Viengkhou, I. L. Campbell and M. J. Hofer, Strawberry notch homolog 2 regulates the response to interleukin-6 in the central nervous system, *J. Neuroinflammation*, 2022, **19**, 126.

142 M. Grill, T. E. Syme, A. L. Nocon, A. Z. Lu, D. Hancock, S. Rose-John and I. L. Campbell, Strawberry notch homolog 2 is a novel inflammatory response factor predominantly but not exclusively expressed by astrocytes in the central nervous system, *Glia*, 2015, **63**, 1738–1752.

143 T. Nakaya, A specific gene-splicing alteration in the SNRNP70 gene as a hallmark of an ALS subtype, *Gene*, 2022, **818**, 146203.

144 T. Nakaya, Dissection of FUS domains involved in regulation of SnRNP70 gene expression, *FEBS Lett.*, 2020, **594**, 3518–3529.

145 H. Bading, Nuclear calcium signalling in the regulation of brain function, *Nat. Rev. Neurosci.*, 2013, **14**, 593–608.

146 B. Granseth and L. Lagnado, The role of endocytosis in regulating the strength of hippocampal synapses, *J. Physiol.*, 2008, **586**, 5969–5982.

147 M. Overhoff, E. De Bruyckere and N. L. Kononenko, Mechanisms of neuronal survival safeguarded by endocytosis and autophagy, *J. Neurochem.*, 2021, **157**, 263–296.

148 M. Manns, O. Leske, S. Gottfried, Z. Bichler, P. Lafenetre, P. Wahle and R. Heumann, Role of neuronal ras activity in adult hippocampal neurogenesis and cognition, *Front. Neurosci.*, 2011, **5**, 18.

149 J. R. Whitlock, A. J. Heynen, M. G. Shuler and M. F. Bear, Learning induces long-term potentiation in the hippocampus, *Science*, 2006, **313**, 1093–1097.

150 Y. Ge, Z. Dong, R. C. Bagot, J. G. Howland, A. G. Phillips, T. P. Wong and Y. T. Wang, Hippocampal long-term depression is required for the consolidation of spatial memory, *Proc. Natl. Acad. Sci. U. S. A.*, 2010, **107**, 16697–16702.

151 T. Sumi and K. Harada, Mechanism underlying hippocampal long-term potentiation and depression based on competition between endocytosis and exocytosis of AMPA receptors, *Sci. Rep.*, 2020, **10**, 14711.

152 H. Blockus, S. V. Rolotti, M. Szoboszlay, E. Peze-Heidsieck, T. Ming, A. Schroeder, N. Apostolo, K. M. Vennekens, P. S. Katsamba, F. Bahna, S. Mannepalli, G. Ahlsen, B. Honig, L. Shapiro, J. de Wit, A. Losonczy and F. Polleux, Synaptogenic activity of the axon guidance molecule Robo2 underlies hippocampal circuit function, *Cell Rep.*, 2021, **37**, 109828.

153 S. B. Arredondo, D. Valenzuela-Bezanilla, M. D. Mardones and L. Varela-Nallar, Role of Wnt Signaling in Adult Hippocampal Neurogenesis in Health and Disease, *Front. Cell Dev. Biol.*, 2020, **8**, 860.

154 M. Soto, W. Cai, M. Konishi and C. R. Kahn, Insulin signaling in the hippocampus and amygdala regulates metabolism and neurobehavior, *Proc. Natl. Acad. Sci. U. S. A.*, 2019, **116**, 6379–6384.

155 A. Kleinridders, H. A. Ferris, W. Cai and C. R. Kahn, Insulin action in brain regulates systemic metabolism and brain function, *Diabetes*, 2014, **63**, 2232–2243.

156 S. Reynhout, S. Jansen, D. Haesen, S. van Belle, S. A. de Munnik, E. Bongers, J. H. Schieving, C. Marcelis, J. Amiel, M. Rio, H. McLaughlin, R. Ladda, S. Sell, M. Kriek, C. Peeters-Scholte, P. A. Terhal, K. L. van Gassen, N. Verbeek, S. Henry, J. Scott Schwoerer, S. Malik, N. Revencu, C. R. Ferreira, E. Macnamara, H. M. H. Braakman, E. Brimble, M. R. Z. Ruzhnikov, M. Wagner, P. Harrer, D. Wieczorek, A. Kuechler,

B. Tziperman, O. Barel, B. B. A. de Vries, C. T. Gordon, V. Janssens and L. Vissers, De Novo Mutations Affecting the Catalytic Calpha Subunit of PP2A, PPP2CA, Cause Syndromic Intellectual Disability Resembling Other PP2A-Related Neurodevelopmental Disorders, *Am. J. Hum. Genet.*, 2019, **104**, 139–156.

157 T. Fanutza, D. Del Prete, M. J. Ford, P. E. Castillo and L. D'Adamio, APP and APLP2 interact with the synaptic release machinery and facilitate transmitter release at hippocampal synapses, *eLife*, 2015, **4**, e09743.

158 N. Khayer, M. Mirzaie, S. A. Marashi and M. Jalessi, Rps27a might act as a controller of microglia activation in triggering neurodegenerative diseases, *PLoS One*, 2020, **15**, e0239219.

159 M. P. Coba, N. H. Komiyama, J. Nithianantharajah, M. V. Kopanitsa, T. Indersmitten, N. G. Skene, E. J. Tuck, D. G. Fricker, K. A. Elsegood, L. E. Stanford, N. O. Afinowi, L. M. Saksida, T. J. Bussey, T. J. O'Dell and S. G. Grant, TNiK is required for postsynaptic and nuclear signaling pathways and cognitive function, *J. Neurosci.*, 2012, **32**, 13987–13999.

160 O. Ostrovskaya, K. Xie, I. Masuho, A. Fajardo-Serrano, R. Lujan, K. Wickman and K. A. Martemyanov, RGS7/Gbeta5/R7BP complex regulates synaptic plasticity and memory by modulating hippocampal GABABR-GIRK signaling, *eLife*, 2014, **3**, e02053.

161 A. McGirr, T. V. Lipina, H. S. Mun, J. Georgiou, A. H. Al-Amri, E. Ng, D. Zhai, C. Elliott, R. T. Cameron, J. G. Mullins, F. Liu, G. S. Baillie, S. J. Clapcote and J. C. Roder, Specific Inhibition of Phosphodiesterase-4B Results in Anxiolysis and Facilitates Memory Acquisition, *Neuropsychopharmacology*, 2017, **42**, 1178.